8-2016

Laboratory and Full Boom-Based Investigation of Nozzle Setup and Restriction Effects on Flow, Pressure and Spray Pattern Distribution

Shane H. Forney
University of Nebraska-Lincoln, shane.forney@huskers.unl.edu

LABORATORY AND FULL BOOM-BASED INVESTIGATION OF NOZZLE SETUP AND RESTRICTION EFFECTS ON FLOW, PRESSURE, AND SPRAY PATTERN DISTRIBUTION

by

Shane H. Forney

A THESIS

Presented to the Faculty of

The Graduate College at the University of Nebraska

In Partial Fulfillment of Requirements

For the Degree of Master of Science

Major: Agricultural and Biological Systems Engineering

Under the Supervision of Professor Joe D. Luck

Lincoln, Nebraska

August, 2016

LABORATORY AND FULL BOOM-BASED INVESTIGATION OF NOZZLE SETUP AND RESTRICTION EFFECTS ON FLOW, PRESSURE, AND SPRAY PATTERN DISTRIBUTION

Shane H. Forney, M.S.

University of Nebraska, 2016

Advisor: Joe D. Luck

Pesticide application is an integral part of crop production and ground-based agricultural boom sprayers are used extensively to apply pesticides to the crop canopy or soil surface across millions of acres in the United States. Efficient application is necessary to minimize costs and limit adverse environmental impacts. Errors in flow rate and system pressure measurements may cause as-applied maps to incorrectly indicate application rates and could negatively affect downstream data processing or analysis.

The goals of this study were to provide quantified measurements on the effects of nozzle setup errors on spray pattern uniformity and evaluate how laboratory patternator data would compare to measurements on a full spray boom. More specific objectives were to: 1) determine the effects from factors such as nozzle lateral angle, nozzle spacing, nozzle replacement and nozzle pitch angle on spray pattern distribution, 2) evaluate a simulation approach to predict the effects of single nozzle boom setup errors on full boom system pattern uniformity, and 3) assess full boom operational measurements (e.g., flow, pressure, and spray pattern) to assess sensitivity for predicting boom distribution errors.

Laboratory and field-based tests were devised to quantify the impact of nozzle setup and operational errors on spray pattern uniformity, boom pressure, and nozzle flow rates. Results indicated that small variations in boom setup or nozzle operation (i.e., pressure or flow) can cause significant errors in spray nozzle distribution which may not be completely detectable by measuring spray pattern alone. Simulations using laboratory data from setup or operational errors reflected similar changes in spray pattern CV as full boom data with similar setup errors. These findings were significant in that it may be possible to model full boom spray distributions based on smaller laboratory-collected datasets. Finally, full boom system-based pressure and flow measurements were compared with similar values at the boom subsection level. Results indicated that localized issues with nozzles or boom subsections may not be readily detected with system-based measurements. Those relying on system-based readings (e.g., pressure or flow) should expect errors exceeding 10% compared to localized measurements across the spray boom.

Dedication

I dedicate this thesis to my family and close friends. Without your support I would not have been able to get to where I am today.

Acknowledgments

The author would like to acknowledge Randy Nuss, Dylan Spatz, Patrick Vanderburg, Adam Barlow and Travis Funseth. These industry partners were integral to the success of the study.

Table of Contents

Figures

Tables

Chapter 1. Introduction

Pesticides, including herbicides, insecticides, and fungicides used to limit yield loss in crops are an integral part of crop production in U.S. agriculture. In the United States over 285 million acres were treated for weeds, grass or brush and over 100 million acres were treated to control insects, according to the 2012 census of agriculture (USDA 2012). In 2014 U.S. producers spent over $15.8 billion on pesticide inputs (USDA 2016). As pesticides are used to treat such large areas, and contribute to such a large portion of input costs, accurate application must be achieved to minimize wasted product.

The fate of agrochemicals (e.g., pesticides and nutrients) has raised concerns regarding risks to human and environmental health. Pesticides pose a threat to humans when encountered in drinking water (Younes and Galal-Gorchev 2000). Excess nutrients in runoff from crop land can enter aquatic ecosystems, increasing the abundance of algae and aquatic plants (Smith et al., 1999), leading to eutrophication. Responsible and efficient application of agrochemicals is important to minimize negative impacts from chemicals not reaching the target pests or crops. Agricultural field sprayers are designed to accurately apply pesticides, fertilizers, and other agrochemicals to the crop canopy, soil surface, or targeted weeds. Proper chemical application requires correct mixing of chemicals, calibration, and selection and setup of that equipment (Grisso et al., 1988).

Chemical application to an unintended area is known as off-target application, which can result in yield loss due to damaged crops and pest pressure. Off-target application generally occurs when field areas are treated two or three times during one application due to overlap of areas sprayed. Sprayers with automatic boom section control and global positioning systems (GPS) aim to minimize overlap and off-target application (Luck et

al., 2010b). Other studies have shown that these systems can greatly reduce over-application, however, pressure fluctuations within the boom due to boom section actuation can be substantial (Sharda et al., 2010). Pressure fluctuations could disrupt the proper rate of chemical application, leading to over- or under-application. Off-rate application occurs when incorrect product rates are applied within a field during spraying, often due to rate controller response or vehicle turning (Luck et al., 2011b).

One method to control the spray application rate is to turn nozzles off and on at varying duty cycles, which is known as pulse width modulation (PWM). Commercially available systems that utilize PWM aim to reduce off-rate application are available from multiple companies including Capstan Ag Systems, Raven Industries, and TeeJet Technologies. PWM nozzle control systems have been evaluated recently by researchers (Porter et al., 2013; Sharda et al., 2013) and shown to compensate flow rate for turns within the ASABE standard for allowable error of 10% coefficient of variation (CV) (ASABE Standards 2011). However, when multiple boom sections were turned off, tip pressures were shown to increase up to 20% and produced a comparable increase in nozzle flow rate (Sharda et al., 2011). Even with these advanced technologies, sprayer boom setup and maintenance can still play a major role in minimizing off-target and off-rate chemical application to entire fields. Individual nozzle spray pattern quality has been shown to decrease with orifice wear (Ozkan et al., 1992). Field operation factors such as boom height, boom roll angle, and boom pitch angle have been investigated (Azimi et al., 1985); however, individual nozzle setup errors and nozzle mounting geometry have not been studied. Therefore, further research regarding the effects of individual nozzle setup errors on sprayer uniformity would be useful.

Chapter 2. Project Goals

A primary goal of this study was to provide quantified measurements on the effects of nozzle setup errors on spray pattern uniformity and evaluate how full boom simulations of laboratory patternator data compare to in-field measurements on a fully operational agricultural sprayer. Additional goals were to evaluate methods of measuring boom pressure, flow rate, and spray pattern distribution. The determination of the effects of errors in system based measurements may lead to the improvement in accuracy of as-applied maps generated from such information.

Chapter 3. Laboratory and Field-Based Investigation of Spray Boom Nozzle Setup Variability Effects on Flow, Pressure, and Spray Pattern Distribution

3.1 Literature review

A field survey of 140 pesticide applicators conducted in Nebraska found that only 1 in 3 liquid pesticide applicators had applied chemicals within 5% of the intended rate (Grisso et al., 1988). Proper application of pesticides is primarily dependent on the operator and his or her competence in equipment selection, calibration and chemical mixing (Grisso et al., 1988). Successful spray application requires that the proper amount of chemical is applied uniformly from the spray boom to the crop or soil surface. Thus, maintaining accurate nozzle flow rates and uniform spray pattern is critical to proper application. If operators understood how boom setup factors influenced spray uniformity (i.e., nozzle flow and spray pattern), they would be better equipped to monitor and correct issues as they developed in the field.

While more challenging than measuring nozzle flow rates, spray pattern testing has been conducted for many years using patternators to evaluate single or multiple nozzle distributions, commonly measured as the coefficient of variation (CV). The effects of orifice wear demonstrated the early use of patternators to quantify nozzle spray pattern performance (i.e., CV) (Ozkan et al., 1992). To minimize human error, computerized spray pattern collection systems have been developed, however, early versions had problems with vibration at some operating conditions (Ozkan and Ackerman 1992). (Luck et al., 2016) built a patternator using digital liquid level sensor technology, capable of measuring spray pattern CVs (in 25 mm increments) and pressure data simultaneously.

Studies have been conducted in the past to quantify the effects that field operation factors might have on pattern uniformity. (Mawer and Miller 1989) studied the effects of boom roll and boom height on spray pattern CV. The findings concluded that boom roll angles as small as one degree could affect the spray pattern CV. A simulation indicated spray pattern CV decreased with increased height (Mawer and Miller 1989), and results from a single nozzle showed that spray pattern CV decreased with increased height (Azimi et al., 1985). Pressure testing of a single nozzle showed decreased spray pattern CV with increased pressure, with the exception of cone and flooding nozzles which showed less improvement with increased pressure (Azimi et al., 1985). Tilt angle (which involved rotating one nozzle) away from the direction of travel was shown to decrease CV, but the investigators warned this may leave spray droplets more susceptible to drift (Azimi et al., 1985). While most studies have focused on how operation (i.e., boom height, tilt, roll, and pressure) of a single nozzle may affect spray uniformity, little has been done to quantify how setup factors of an individual nozzle among a boom of properly mounted nozzles might contribute to the spray distribution of the system. For instance, a single nozzle tilted laterally or fore or aft may have a negative impact on the spray pattern. The effects of improper nozzle spacings within a boom section on pattern uniformity have also not been previously reported.

3.2 Goals and objectives

The goals of this study were to provide quantified measurements on the effects of nozzle setup errors on spray pattern uniformity and evaluate how laboratory patternator data would compare to measurements on a full spray boom. More specific objectives were to: 1) determine the effects from factors such as nozzle lateral angle, nozzle spacing, nozzle

replacement and nozzle pitch angle on spray pattern distribution, 2) evaluate a simulation approach to predict the effects of single nozzle boom setup errors on full boom system pattern uniformity, and 3) assess full boom operational measurements (e.g., flow, pressure, and spray pattern) to assess sensitivity for predicting boom distribution errors.

3.3 Materials and Methods

Spray pattern distribution, boom pressure, and nozzle flow rates were collected on a patternator, as outlined by (Luck et al., 2016), to quantify how nozzle setup errors may impact spray distributions. The patternator was constructed per ASTM standard E641-01 (ASTM 2006) and was capable of simultaneously recording spray pattern distribution in 25 mm increments and pressure data at the nozzle (Figure 3.1). To measure spray pattern CV, the patternator measured the amount of time to fill a fixed volume for each 25 mm division. As each individual tube was filled, a liquid-level sensor triggered a virtual instrument (VI) in LabVIEW (National Instruments Corporation, Austin, TX) and a flow rate for each 25 mm division was automatically recorded.

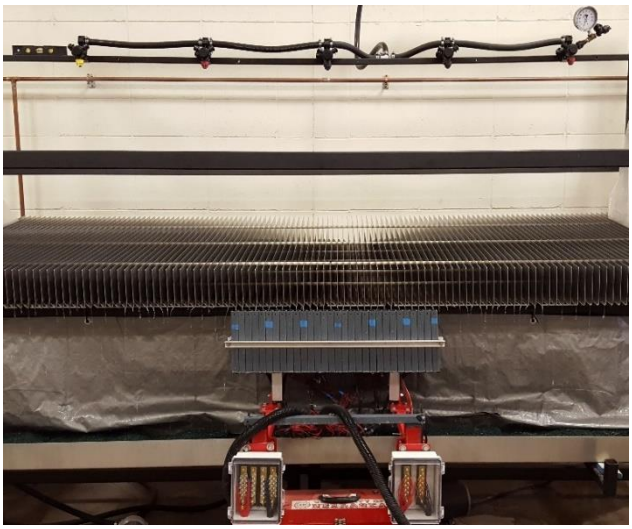

Figure 3.1. Spray table as outlined by Luck et al (2016) for automatic spray pattern data collection.

The software generated a spreadsheet and provided a quantitative and visual depiction of the spray pattern. Spray pattern quality was quantified by CV, defined as standard deviation divided by the mean, as calculated by Equation 3.1 (Ozkan et al, 1992). CV is a standardized measure of the dispersion of data points, and when applied to spray patterns it measures how evenly nozzle effluent is distributed. Higher CVs indicate a poor or uneven spray distribution while lower CVs indicate improved uniformity.

$$CV(\%) = (100\%) \cdot \sqrt{\frac{\sum_{i=1}^{n}(x_i - \bar{x})^2}{n-1}} \Bigg/ \frac{\sum_{i=1}^{n} x_i}{n} \qquad \text{Equation 3.1}$$

Where:

x_i =flow rate (fixed volume divided by the time to fill the tube) of i^{th} sample tube across spray pattern width (mL min^{-1}),

$\bar{x}$ = mean flow rate (mL $\cdot$ min^{-1}) to fill tubes across pattern width,

n = number of samples.

Tests using the indoor patternator system took place at the University of Nebraska-Lincoln Sprayer Research lab, free of wind or other environmental conditions. Nozzles used during this study were extended range (XR) flat fan nozzles and air injected extended range (AIXR) flat fan nozzles (TeeJet Technologies 2015) manufactured by TeeJet (TeeJet Technologies, Wheaton, Ill.). The aforementioned nozzles were chosen because they are common nozzles used in pesticide application in the U.S.

3.3.1 Nozzle Lateral Angle Test

The nozzle lateral angle test setup consisted of five nozzles mounted above the patternator in a dry boom configuration. A system is considered a dry boom configuration if the support mechanism and spray solution delivery mechanism are separate, whereas in

a wet boom configuration the support mechanism also delivers the spray solution (Klein 2004). Spray distribution measurements were recorded as the center nozzle was rotated in a clockwise direction about a horizontal axis perpendicular to the boom in 2° increments from 0° to 8° (Figure 3.2) while the surrounding nozzles remained stationary.

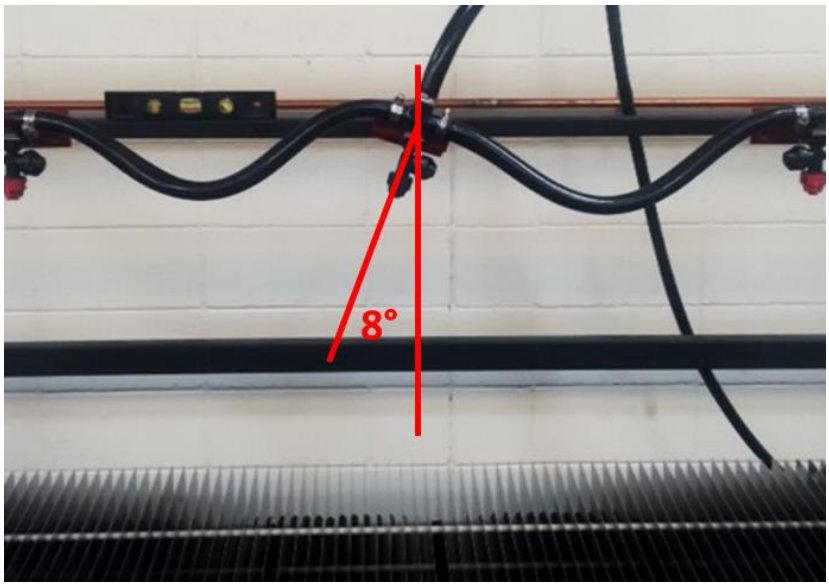

Figure 3.2. Nozzle lateral angle test with test nozzle set to 8° (not to scale).

Spray pattern data were collected in two 76 cm sets to the left and right of the center nozzle, and were combined to make one 152 cm dataset at each angle setting. Three replicates of 152 cm spray pattern data were collected for each treatment. Tests were run first with TeeJet XR8003 nozzles, then XR8005 nozzles, placed 76 cm above the spray table on 51 cm spacings, as recommended by the manufacturer (TeeJet Technologies 2015). The system pressure was set to 207 kPa via a pressure relief valve (23120, TeeJet Technologies, Wheaton, Ill.). Additional tests were recorded using XR11003 and AIXR11003 nozzles placed 51 cm above the patternator surface at 51 cm spacings. The XR11003 nozzles were tested at a system pressure of 207 kPa while the AIXR11003 nozzles were tested at 207 and 345 kPa. It should be noted that the air injected (AIXR

series) nozzles were operated at two different pressures, as the AIXR nozzle operating pressure is much higher than the operating pressure of the XR nozzles (TeeJet Technologies 2015). Nozzle spacing, boom height, and system pressure remained unchanged as the lateral angle was adjusted during these tests. Test results were analyzed for significant differences using a general mixed model (GLIMMIX) in SAS v9.4 to run a Least Significant Means (LSM) test (SAS Institute Inc. 2013) with an alpha level of 0.05. The LSM test was setup using the lateral angle settings as treatments to determine which lateral angle settings produced significantly different spray pattern distributions.

3.3.2 Nozzle Spacing Test

To test for the effects of improper nozzle spacings, six XR8003 nozzles, 76 cm above the table at 51 cm spacings, were set up above the patternator surface and operated at 207 kPa. Additional tests were conducted with six AIXR11003 nozzles, 51 cm above the table at 51 cm spacings and at an operating pressure of 345 kPa. Nozzles were assigned numbers one through six from left to right, and nozzle number three was offset in 25 mm increments to the right (Figure 3.3). Data were collected for nozzle number three with offset values of 0, 25, 50, 75, 100 and 125 mm. The patternator was positioned to collect two sets of 76 cm of pattern data to the right and left of the third nozzle, combined to make one 152 cm dataset centered beneath the original location of the third nozzle. Three replications of spray pattern data were taken for each offset value. A LSM test, with an alpha of 0.05, was used to determine differences among the mean spray pattern CV for the nozzle offset values.

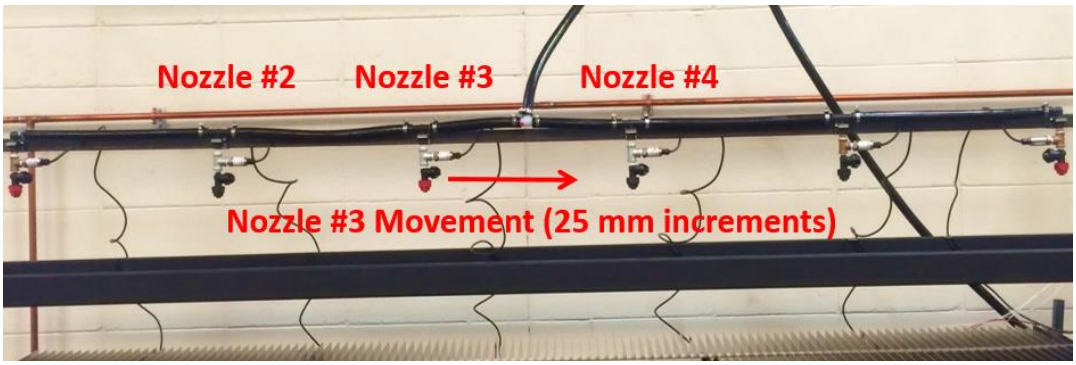

Figure 3.3. Nozzle spacing test with nozzle three, as shown, moved in 25 mm increments to the right.

3.3.3 Nozzle Replacement Test

To test for the effect due to an incorrect nozzle placed within the spray boom, six TeeJet XR8003 nozzles were placed 76 cm above the spray patternator surface, at 51 cm spacings, and at an operating pressure of 207 kPa. A baseline spray pattern measurement (152 cm centered below the third nozzle) was established with three replications of the six XR8003 nozzles. To test the effect due to either an incorrect nozzle or a worn nozzle, the third nozzle (from left) was replaced with an XR8001 and then an XR8005 nozzle. Three replications of spray pattern data were collected with both nozzle replacements. Boom pressure was monitored with calibrated pressure transducers (PX309-100G5V, Omegadyne, Inc., Sunbury, Ohio). The pressure transducers produced a 0-5V DC output directly proportional to 0-690 kPa (100 PSI) pressure range. Flow rate data were manually collected from all six spray nozzles during each test using a graduated cylinder with graduations in increments of 2 mL and a stopwatch. To estimate effects on spray pattern uniformity or nozzle flow rates from these changes, the spray pattern CVs from the tests with XR8001 and XR8005 nozzles were compared to CVs from the XR8003 nozzles. In addition to spray pattern distribution, nozzle flow rates were recorded and compared.

3.3.4 Nozzle Pitch Angle Test

To evaluate effects of nozzle pitch angle on pattern uniformity, five XR11003 nozzles were placed 51 cm above the patternator in 51 cm spacings and the system pressure was set to 276 kPa. The center nozzle was rotated about a horizontal axis parallel to the boom in 4° increments from 0° to 24° first clockwise, then counterclockwise, when the boom was viewed from the right side (Figure 3.4). The other four nozzles remained pointed vertically downward above the patternator. Three replications of data were recorded for each nozzle setting. A LSM test with an alpha value of 0.05 was used to determine significant differences among the CVs produced by the nozzle settings.

Figure 3.4. Nozzle pitch angle test with nozzle rotated 8° counterclockwise from vertical (not to scale).

3.3.5 Comparison of Laboratory Simulated Pattern Data versus Full Boom Field Pattern Test

Spray pattern data from one replicate of the laboratory patternator tests (152 cm widths) were extrapolated to simulate the full boom of a sprayer. Baseline data sets of XR8003 spray pattern and boom pressure were used to simulate a 27.4 m spray boom. One set of

baseline 152 cm spray pattern data was then removed and replaced with 152 cm of spray pattern data from the nozzle replacement test (i.e., the XR8003 and XR8005 nozzle replacements). These tests were conducted to quantify the effect of a single nozzle setup error on a full boom width. To observe the effects of spray pattern collection width increments, the data collected in 25 mm width increments during the nozzle lateral angle test were grouped into 100 mm increments by averaging flow rates from four 25 mm collection width increments. The effects of spray collection width were quantified to determine if the laboratory patternator data could be compared to full boom sprayer pattern data, which was collected in 100 mm widths.

To document the effectiveness of boom plumbing layout, nozzle spacing measurements were taken to the nearest 1.51 mm (1/16 in) between successive nozzle bodies and nozzle tips. A common point in the middle of each nozzle body (top of the arrow in Figure 3.5) was used as the location for measuring this spacing. For this spray boom the ideal spacing was 51 cm. Distances between nozzle tips were also measured using the same method. The distance from the center of rotation to the nozzle tip (60 mm) was used to calculate nozzle lateral angle deviations. A simulation spray pattern was created using lateral angle test results corresponding to rotation angles measured from nozzle body and tip spacings. The result was a modified baseline simulation that accounted for nozzle tip and spacing deviations along the boom.

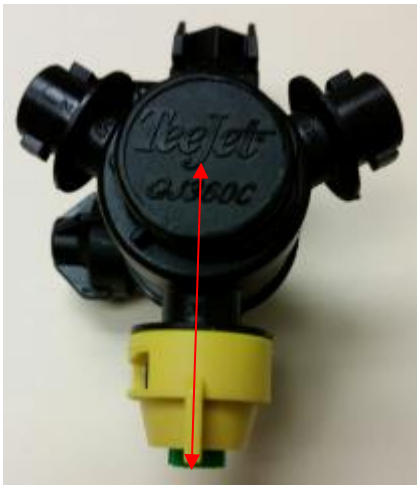

Figure 3.5: TeeJet QJ360C nozzle bodies used on Apache sprayer during outdoor boom tests. The distance from nozzle tip to center of rotation, as shown by red arrow, is 60 mm.

Spray pattern, boom pressure, and nozzle flow rate data were collected on a full boom sprayer to compare with the full boom simulations. An Apache AS1020 self-propelled sprayer with a 27.4 m boom (54 nozzles at 51 cm spacing) was used in conjunction with a mobile patternator (Sprayertest 1000, Herbst pflanzenschutztechnik, Hirschbach, Germany) to collect spray pattern data. The Herbst Sprayertest 1000 (Figure 3.6) is a mobile patternator in which the user places a track underneath the spray boom and installs the spray pattern collection cart on the track. The cart used 100 mm collection troughs to collect spray pattern data, recording the spray pattern data 1 m at a time.

Figure 3.6: Herbst Sprayertest 1000 on tracks placed below Apache AS1020 sprayer, with the spray pattern collection device installed on the end of the tracks (foreground of picture).

The spray pattern collection cart had a control software for the user to enter the start and end positions of the spray boom and the spray pattern collection cart moved to the start location and recorded a spray pattern measurement starting at the centerline of the first nozzle, then automatically moved one width of the collection table down the track to record the next spray pattern distribution measurement. Individual spray pattern measurements were recorded in this manner until reaching the centerline of the last nozzle. After all the individual spray pattern measurements were recorded, a composite of the spray pattern measurements was compiled and exported to an Excel document. Boom pressure data were collected using both electronic pressure transducers (Omega Engineering PX309-100G5V) installed inline within the boom hose (Figure 3.7), and a manual pressure gauge fitted to a nozzle body connector (Figure 3.8).

Figure 3.7: Omega pressure transducer plumbed in line with boom subsection supply line.

The output signal from the electronic pressure transducers was recorded to a .txt file at 1 Hz using a microcontroller (Arduino Mega 2560, Arduino LLC, Ivrea, Italy). The manual pressure gauge (PGS-35L-100, Omegadyne, Inc., Sunbury, Ohio) had a minimum graduation increment of 6.9 kPa (1 psi) for taking pressure readings (Figure 3.8).

Figure 3.8: Nozzle pressure gauge (graduations in increments of 6.9 kPa) used for manual individual nozzle pressure measurements.

A diagram of the spray boom is illustrated in Figure 3.9 showing locations of the pressure transducers. Nozzle flow rates were collected using a 250 ml graduated cylinder (graduations in increments of 2 mL) and a stopwatch. Three replicates of flow rate measurements were taken at each nozzle across the boom during the tests.

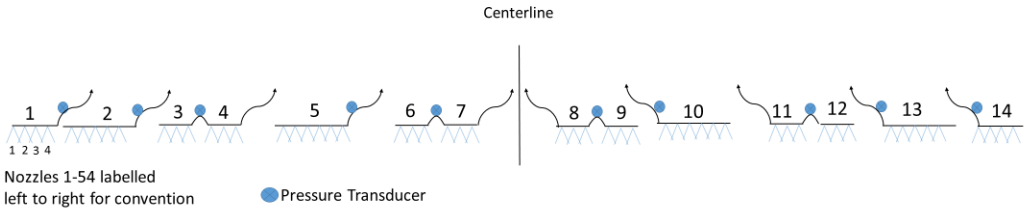

Figure 3.9: Boom setup diagram of Apache AS 1020 showing boom subsections and pressure transducer placement.

The data collected using the laboratory patternator in 25 mm collection width increments were grouped into 100 mm collection width increments by averaging flow rates from four 25 mm collection width increments. Since the Sprayertest 1000 utilized 100 mm collection width increments, it was necessary to convert the simulated full boom data from the laboratory patternator to 100 mm collection width increments so the patterns were on an equal basis for comparison. The baseline test of full boom pattern data utilized XRC8003 nozzles with the boom positioned 76 cm above the surface of the Sprayertest 1000. The operating pressure was set to 207 kPa on the Raven in-cab monitor. The nozzle at position 20 (numbered from left to right), in the fourth boom subsection (Figure 3.9) was replaced with an XR8001 and then an XR8005 nozzle for the two subsequent nozzle replacement tests. Three replicates of pattern and pressure data (both manual and automated pressure sensor data) were collected along with flow rate data. Comparisons were then made between the modified baseline simulation and the full

boom baseline data along with replacements of the XR8001 and XR8005 nozzles between simulations and actual data collected with the mobile patternator.

3.4 Results and Discussion

3.4.1 Nozzle Lateral Angle Test

Figure 3.10 shows the spray pattern distribution from replicate 1 of the nozzle lateral angle test baseline (0° nozzle lateral angle), which yielded a CV of 4.1%. The x-axis shows each 25 mm patternator collection width (numbered 1 to 60 as a position identifier). The center nozzle was positioned between volume divisions 30 and 31. Figure 3.11 shows the spray pattern distribution when the test nozzle (nozzle #3) was rotated 8° to the left. The histogram shows that the flow rates on the left side of the patternator, the side towards which the nozzle was rotated towards, were higher than on the right side. The spray pattern shown in Figure 3.11 was from replicate 2 with the 8° clockwise nozzle lateral angle which had a CV of 15.4%, and was visibly worse than that of the baseline distribution shown in Figure 3.10.

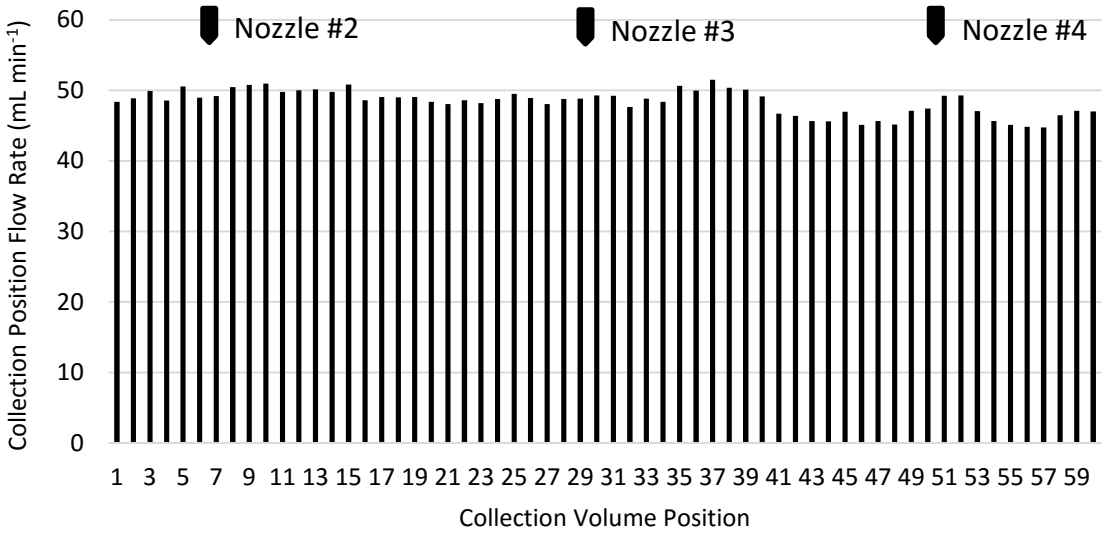

Figure 3.10. Spray pattern from nozzle lateral angle test in flow rate versus position with 0° of nozzle lateral angle rotation using XR8003 nozzles (76 cm height, 51 cm spacing, 207 kPa).

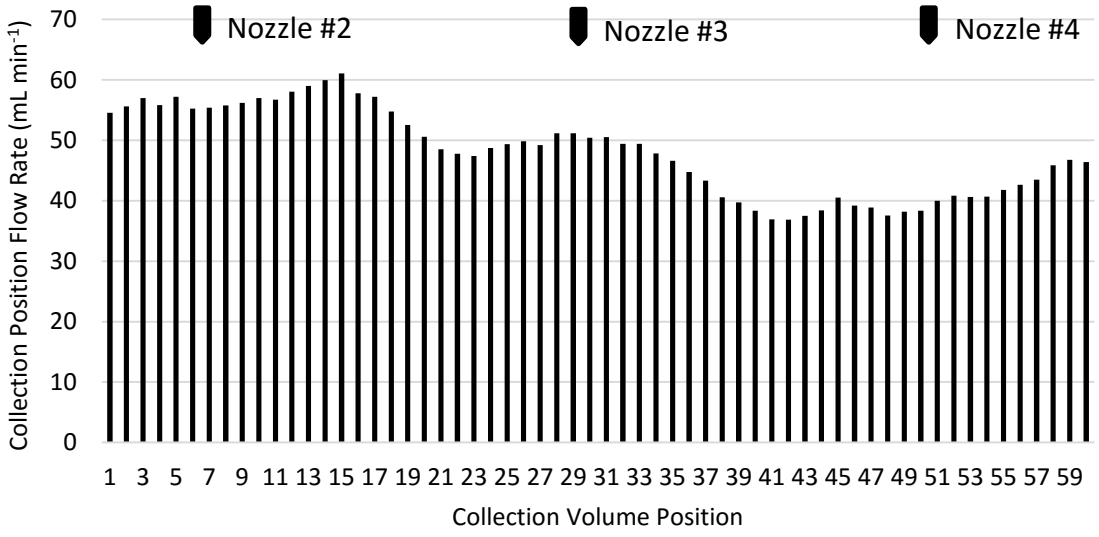

Figure 3.11. Spray pattern from nozzle lateral angle test in flow rate versus position where nozzle #3 was rotated 8° clockwise using XR8003 nozzles (76 cm height, 51 cm spacing, 207 kPa).

The baseline CV (i.e., 0° center nozzle lateral angle for XR8003 nozzles, 76 cm height, 51 cm spacing, and operating at 207 kPa), averaged 4.2%. The baseline test with XR8005 nozzles had an average CV of 5.1%. The threshold for a desirable pattern was considered

at a CV below 10% (Ozkan et al., 1992; Azimi et al., 1985). As the lateral angle rotation of the center nozzle of the pattern increased, the CVs also tended to increase (Table 3.1). The results for the 80° nozzles (XR8003 and XR8005) showed that as the nozzle angle reached 4° CV values approached 10%. With a nozzle lateral angle of 8°, the CV for both 80° nozzles exceeded 15%, which would be considered unacceptable (Ozkan et al., 1992). Statistical analysis revealed that each 2° increment in nozzle lateral angle significantly ($p \leq 0.05$) increased the average spray pattern CV for XR8003 and XR8005 nozzles (Table 3.1). The nozzle lateral angle test data for the 110° nozzles is also summarized in (Table 3.1). The baseline CV for the XR11003 averaged 6.5% while baseline CVs for the AIXR11003 nozzles at 207 and 345 kPa were 10% and 4.5%, respectively. These data indicated that pattern uniformity of flat fan nozzles with 110° spray angles was less susceptible to nozzle lateral angle changes than the 80° nozzles. The narrower nozzle fan angles and higher boom heights, of 80° nozzles compared to 110° nozzles, likely contributed to the larger CV deviations at smaller lateral angle changes. The AIXR operating at 207 kPa had much higher CVs than those of the AIXR nozzles operated at 345 kPa (Table 3.1).

Table 3.1: Summary of nozzle lateral angle test CV results for five nozzles.

Center Nozzle Lateral Angle	XR8003 [76 cm height at 207 kPa] (%)	XR8005 [76 cm height at 207 kPa] (%)	XR11003 [51 cm height at 207 kPa] (%)	AIXR11003 [51 cm height at 207 kPa] (%)	AIXR11003 [51 cm height at 345 kPa] (%)
0°	4.2[a]	5.1[a]	6.5[a]	10.0[a]	4.5[a]
2°	5.3[b]	8.0[b]	6.6[a]	9.9[a]	4.9[a]
4°	9.9[c]	11.1[c]	7.2[a]	10.2[b]	6.0[b]
6°	11.5[d]	12.7[d]	7.5[a]	10.9[b]	6.2[b]
8°	15.6[e]	18.1[e]	7.9[a]	11.5[c]	8.4[c]

[†]Within each nozzle, mean CVs with same letter were not significantly different ($p \leq 0.05$). Mean CVs between nozzles were not tested for significant difference.

Interestingly, as the nozzle lateral angle increased, the CVs for the XR11003 nozzles increased, but at a lower rate than for the XR8003 nozzles (Table 3.1). The average CV for the first increment of nozzle angle rotation (2°) increased slightly, and at the largest angle rotation (8°), the average spray pattern CV had only increased to 7.9%. Each nozzle rotation increment was significantly different for the 80° nozzles, XR8003 and XR8005, while none of the rotation increments resulted in significantly different spray patterns CVs with the XR11003 nozzles. The results in Table 3.1 clearly show the average spray pattern CV for the 110° nozzles (XR11003, AIXR11003) was less affected by nozzle rotation compared to the 80° nozzles (XR8003, XR8005).

3.4.2 Nozzle Spacing Test

Results from the nozzle spacing test showed that changing the middle of three XR8003 nozzle's position (spacing) by as much as about one-fourth of the initial spacing did not raise the CV above the 10% level where CV was considered unacceptable (Table 3.2). As shown in Table 3.2, baseline CVs for both 80° and 110° nozzles at a 51 cm spacing were established at 3.8% and 4.9%, respectively. As nozzle #3 was moved to the right in 25 mm increments, the spray pattern CV values increased. Considerable deviations in nozzle spacing occurred before undesirable pattern CVs (i.e., greater than 10%) were noticed with these nozzle configurations. For both nozzle sets there was no significant change from the initial 51 cm spacing CV until the nozzle was moved 50 mm to the right (Table 3.2). Each subsequent increment of movement to the right produced an increase in CV for both nozzles, however, the spray pattern CVs did not exceed 10% until both nozzle sets had been moved 125 mm to the right. These results indicate that the spray pattern for 80°

and 110° nozzles did not change significantly until the spacing deviation along the boom increased above one-tenth of the original spacing.

Table 3.2. Summary of nozzle spacing test CVs as nozzle #3 moved to the right in 25 mm increments from original 51 cm spacing.

Nozzle #3 Offset (mm)	XR8003 CV† (%)	AIXR11003 CV† (%)
0	3.8[a]	4.9[a]
25	4.7[a]	4.8[a]
50	6.2[b]	5.5[b]
75	7.7[c]	6.8[c]
100	8.0[c]	9.4[d]
125	11.1[d]	11.4[e]

†Mean CVs with same letter were not significantly different ($p \leq 0.05$).

3.4.3 Nozzle Replacement Test

Baseline data were collected using six XR8003 nozzles and produced an average spray pattern CV of 4.1% with individual replicates as low as 3.9%. Spray pattern CVs increased to 18.9% and 8.4% when the original XR8003 #3 nozzle was replaced with an XR8001 and then an XR8005 nozzle, respectively (Table 3.3). Flow rate changes (measured in % change from the 16.7 $mL \cdot s^{-1}$ baseline of all XR8003 nozzles) from the replacement tests were much larger than changes in the spray pattern CV. When the XR8001 nozzle replaced the XR8003 nozzle, the spray pattern CV increased by 14.8% while the test nozzle flow rate decreased by 66%. The XR8005 replacement resulted in a 4.3% increase in spray pattern CV while the flow rate increased by 70% relative to the XR8003 nozzle flow rate. These results demonstrate that replacement of incorrect nozzles (or nozzle plugging or wear) can adversely impact both flow rate and spray pattern CVs. It should be noted that nozzle flow rate deviations (% flow) were much larger than changes in spray pattern CVs. High flow rate changes occurred before pattern CVs began to increase above the 10% unacceptable level.

Table 3.3. Summary of average (of three replicates) spray pattern CV, flow rate changes and pressure from nozzle replacement test.

Nozzle at Position #3	Average (of three replicates) Spray Pattern CV (%)	Nozzle #3 Flow Rate ($mL \cdot s^{-1}$)	Flow Deviation from XR8003 (%)	Average boom pressure (kPa)
XR8001	18.9	5.6	- 66	209.1
XR8003	4.1	16.6	-	209.8
XR8005	8.4	28.0	+ 70	205.6

3.4.4 Nozzle Pitch Angle Test

Table 3.4 summarizes the results for the nozzle pitch angle test. The baseline spray pattern CV for the pitch angle rotation forward of vertical (fore) averaged 5.0%. The spray pattern CV remained at 5.6% for the 4°, 8°, and 12° fore rotations and averaged 7.1% at 24° of fore rotation. The spray pattern CV for the aft rotation averaged a baseline CV of 4.9% and an average spray pattern CV of 4.8% with a nozzle pitch angle rotation 4° aft of vertical. The spray pattern CV increased with each increment of nozzle pitch angle rotation thereafter. The largest spray pattern CV averaged 8.9% at 24° of nozzle pitch angle rotation aft of vertical. This shows that fore/aft rotation of the middle of the three nozzles up to 24° from vertical did not increase spray pattern CV above the maximum desirable CV limit of 10%.

Table 3.4. Summary of nozzle pitch angle test with XR11003 nozzles rotated about a horizontal axis parallel to the boom.

Center Nozzle Pitch Angle	Spray Pattern CV† Fore of vertical (%)	Spray Pattern CV† Aft of vertical (%)
0°	5.0[a]	4.9[a]
4°	5.6[a,b]	4.8[a]
8°	5.6[a,b]	5.6[b]
12°	5.6[a,b]	6.5[c]
16°	5.9[b]	7.5[d]
24°	7.1[c]	8.9[e]

†Mean CVs with same letter were not significantly different ($p \leq 0.05$).

3.4.5 Comparison of Laboratory Simulated Pattern Data versus Full Boom Field Pattern Test

Figure 3.12 shows a simulation of 27.4 m data (of XR8003 nozzles) with a CV of 3.8%. This represented a well-balanced boom with adequate flow and positioning from all nozzles.

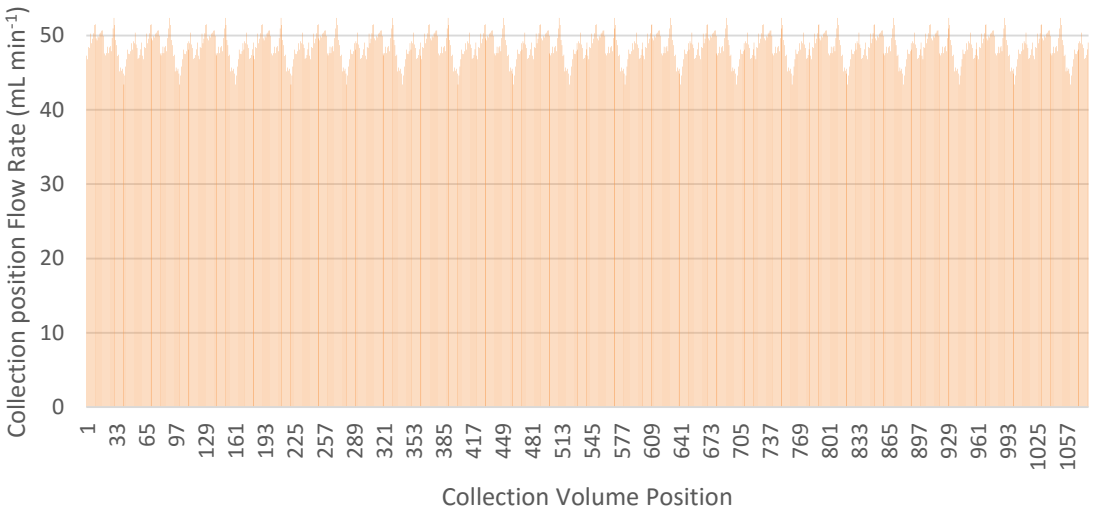

Figure 3.12: Simulation of 27.4 m boom of XR8003 nozzles using 152 cm spray pattern data (CV 3.8%)

To simulate the effect of having a nozzle obstruction in the 27.4 m boom simulation 152 cm of pattern data were replaced with 152 cm of data from the nozzle replacement test using an XR8001 nozzle (Figure 3.13). The simulated boom represents how the pattern may perform if one of the proper nozzles (XR8003) were to be replaced with a smaller nozzle (XR8001). The CV from the simulated boom with the smaller nozzle replacement was 7.6%. This change produced an increase in CV from the well-balanced boom in Figure 3.11. The simulated full boom CV was much lower than the resulting CV from the 152 cm patternator CV with an XR8001 in one nozzle position (18.9%) Table 3.3. This

showed that CV is much more sensitive when calculated from three nozzles as opposed to a full boom width of 54 nozzles.

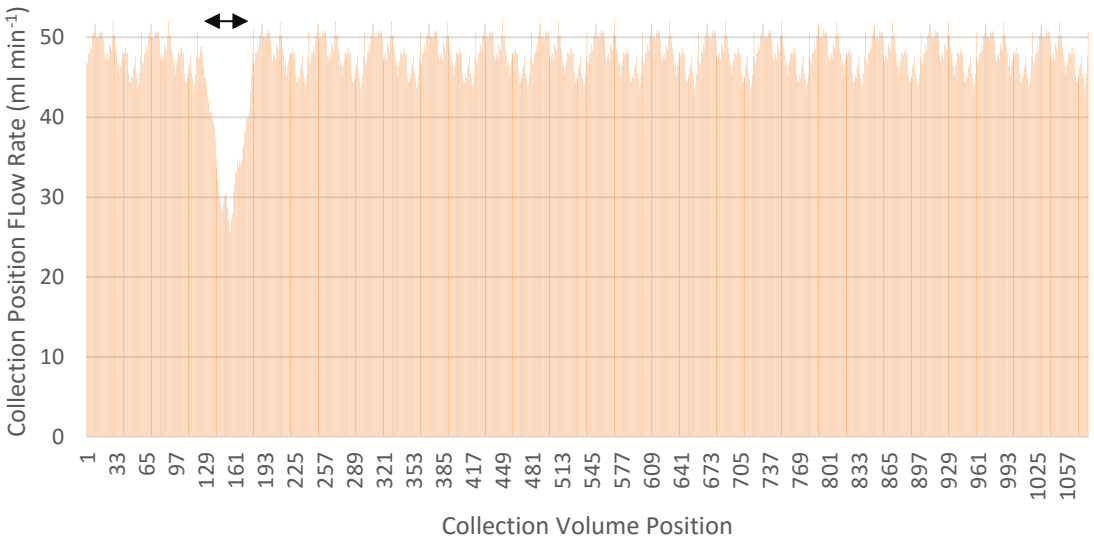

Figure 3.13: Simulation of 27.4 m boom of XR8003 nozzles using 152 cm spray patternator data (CV 7.6%) with XR8001 nozzle at collection position indicated with arrow.

To simulate the effects of a worn nozzle within the full boom simulation, the same process was performed using the XR8005 nozzle data that was originally contained in (Table 3.3). The 27.4 m boom simulation with this 152 cm section of data is shown in Figure 3.14. The resulting CV (7.3%) represented an increase from the 3.9% baseline CV using a full boom simulation of XR8003 nozzles. The CV increase was not as large in the 27.4 m situation when compared to the 152 cm data set, which produced a CV of 8.4% (Table 3.3). As stated before, the increase in CV was smaller in full boom situations than in data sets of three nozzle spacings.

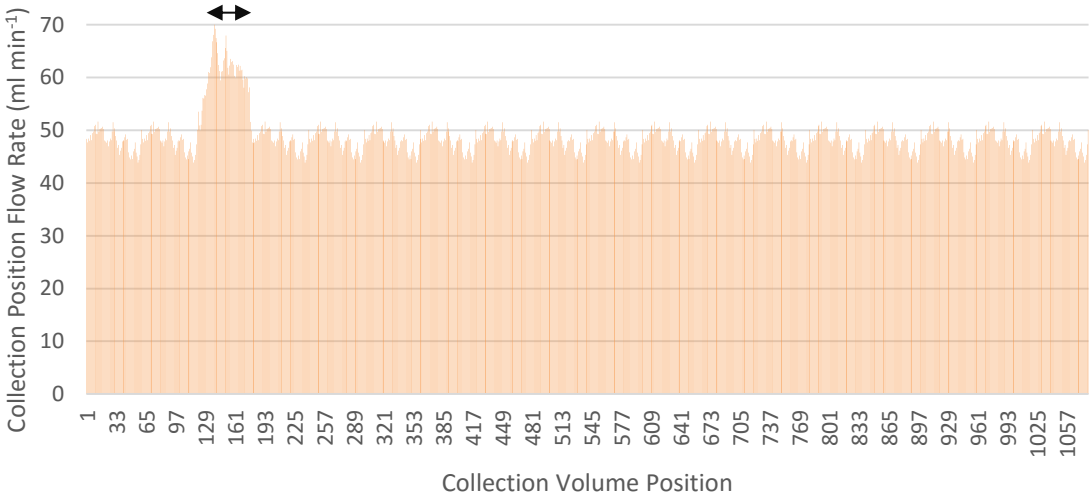

Figure 3.14: Simulation of 27.4 m boom of XR8003 nozzles using 152 cm spray patternator data (CV 7.3%) with XR8005 nozzle included at the position indicated by an arrow.

As previously discussed, direct comparisons between laboratory patternator data and the full boom system required modification of the laboratory data so spray pattern collection widths were equal. Patternator data in 25 mm collection width, from the nozzle lateral angle test, were averaged into 100 mm collection widths. Figure 3.15 graphically depicts the CV from lateral angle test in both 25 mm collection width increments and 100 mm averaged collection widths. The effect from collection width was minimal with the largest difference in CV being 0.2% (Table 3.5). This showed that the simulation data could be converted from 25 mm collection widths to 100 mm collection widths with negligible affects to the CV values.

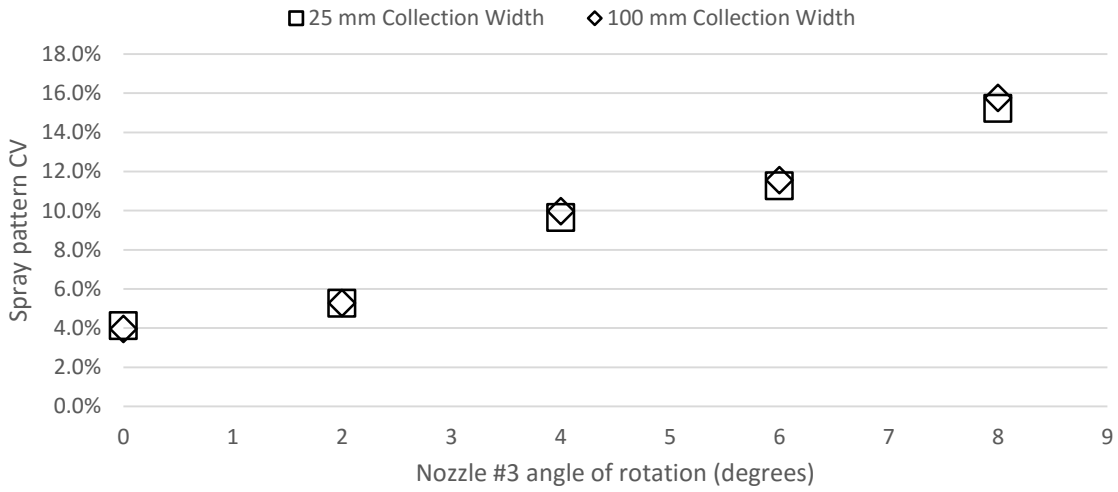

Figure 3.15: Twenty five mm pattern results from nozzle lateral angle test averaged into 100 mm collection widths.

Table 3.5: Spray pattern CVs results from 25 mm nozzle lateral angle test averaged into 100 mm collection widths.

Nozzle #3 Lateral Angle Rotation (degrees)	Spray Pattern CV for 25 mm collection width	Spray Pattern CV for 100 mm collection width
0	4.1%	3.9%
2	5.3%	5.2%
4	9.6%	9.7%
6	11.3%	11.3%
8	15.2%	15.4%

Figure 3.16 shows the results of the averaging when applied to the simulation. The conversion demonstrated only a slight (0.4%) decrease in average spray pattern CV as compared to the 27.4 m boom simulation with 25 mm collection widths (Figure 3.12). Therefore, the data averaged into 100 mm collection widths was suitable for comparison to the full boom data. The resulting spray patterns from larger collection width were repeated to form a simulated 27.4 m boom to be compared to the spray distribution from the full boom spray pattern test results.

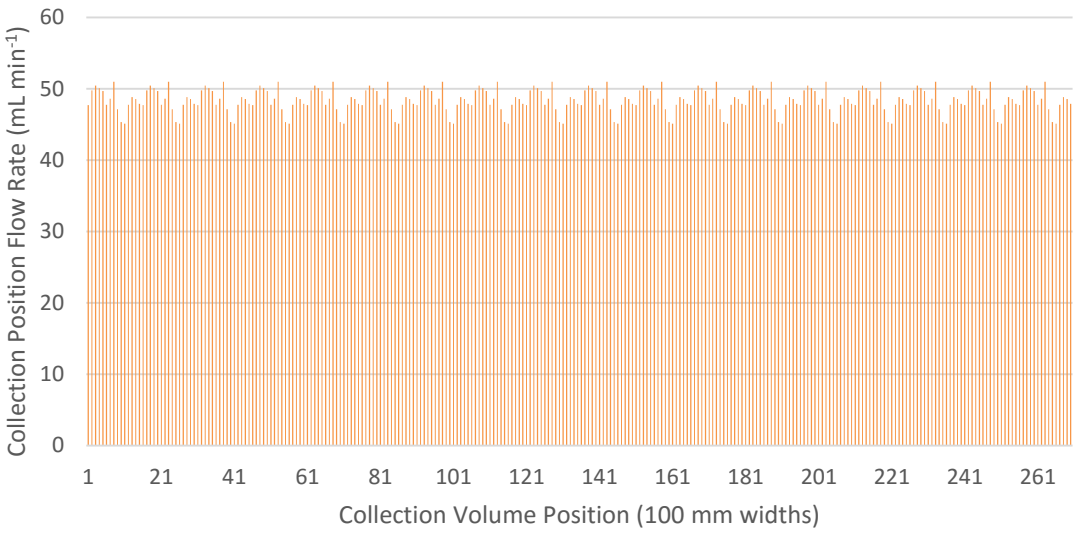

Figure 3.16: Simulation of 27.4 m boom of XR8003 nozzles using 152 cm spray patternator data (25 mm collection width) grouped into 100 mm collection widths (CV 3.4%)

The baseline spray pattern data collected from the full boom sprayer using the Sprayertest 1000 is shown in Figure 3.17. A summary of the boom pressure, flow rates, and spray pattern results from the sprayer can be found in Table 3.6. Flow rate data from all nozzles were compared to the average flow across the boom and found to be within 5% from the average flow rate. Thus, initial nozzle flow rate CVs (prior to any treatments) were fairly consistent and low. The baseline performance data for the sprayer resulted in a pattern CV of 11.0% which was much higher than anticipated for the system. Manual pressure readings at each nozzle showed little variation (for the XR8005 nozzle, no pressure deviation was noticed with the manual pressure gauge). When the nozzle at position #20 was changed from the XRC8003 to the XR8001 and XR8005 nozzles, changes were apparent in the pattern and flow rate data. In both cases, there were small increases in overall spray boom CV, while much larger changes were noticed in nozzle flow rate CV values for the entire boom. Variations in pressure among nozzles or boom sections were negligible.

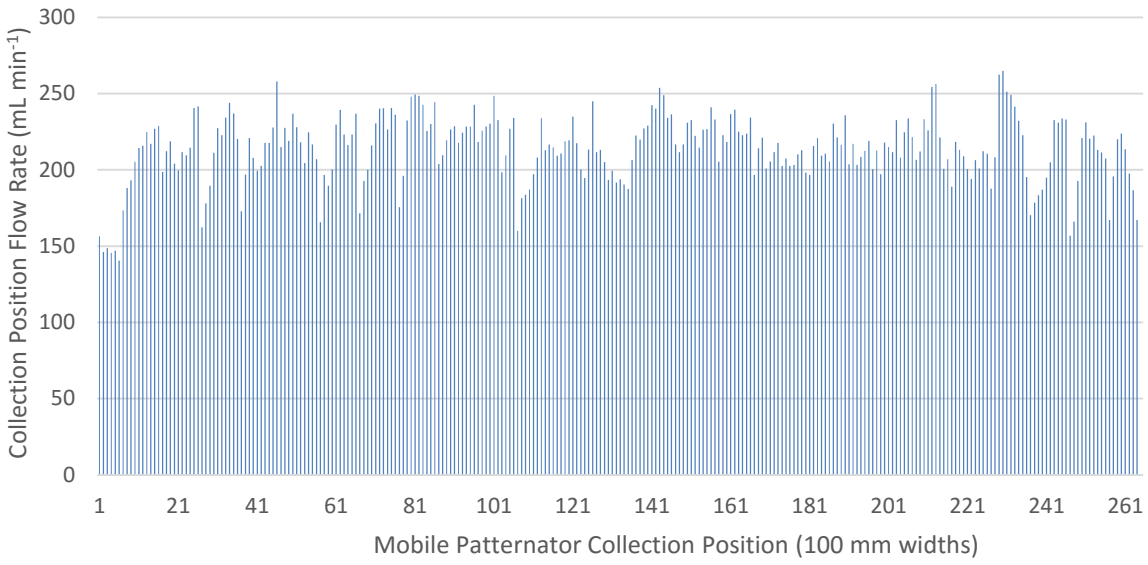

Figure 3.17: Mobile spray patternator output for baseline full boom data collection (11% CV).

Table 3.6: Summary of spray pattern, nozzle pressure, boom section pressure and nozzle flow rate CV data for nozzle #20 replacement tests.

Test Setup	Average Spray Pattern CV (%)	Average Nozzle Pressure CV (%)	Average Boom Section Pressure CV (%)	Average Nozzle Flow Rate CV (%)
Baseline	11.0	1.9	1.0	1.4
w/ XRC8001	13.3	2.7	0.8	9.1
w/ XRC8005	12.3	-	0.8	8.5

A large discrepancy was noticed between the simulated 27.4 m boom baseline (3.4% CV) and the data collected from the mobile patternator (11% CV). The baseline pattern starting much higher, where more variation has a smaller impact. The simulation starts with a much lower baseline CV, therefore, any variation introduced would cause a larger increase in CV. To explain the high initial CV of the full boom spray pattern, some factors were considered which may have contributed to the spray pattern uniformity. Because few issues were noticed with boom pressure and flow measurements during baseline tests, nozzle spacing measurements were observed to determine if they may have

affected the high pattern CV measured (11%). Summing the 53 nozzle body spacing or the 53 nozzle tip spacing measurements revealed an error of only +5 cm in total boom width in either case. Figure 3.18 shows a histogram of nozzle body spacing deviations (in mm) from the ideal spacing of 50.8 cm. Of the total 53 spaces between nozzle bodies along the boom, 32 deviated by less than ±5 mm. Fourteen spacing deviations varied between ±5 to 10 mm while another six nozzle bodies spacing deviations exceeded ±10 mm. Only one spacing measurement indicated a deviation greater than 20 mm, measured at 48.6 mm.

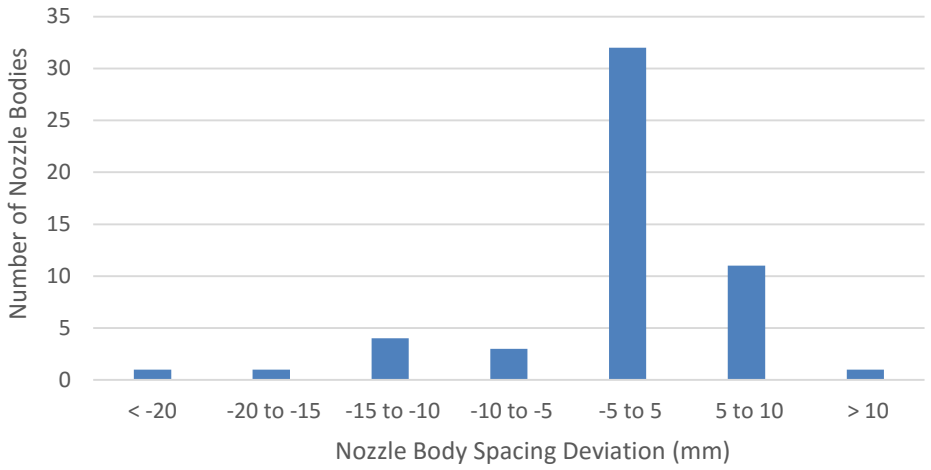

Figure 3.18: Number of nozzle body spacings at various deviations (mm) from ideal spacing of 50.8 cm.

Based on the information contained in Table 3.1, the differences in nozzle body spacings that exceeded 20 mm could have affected spray pattern CV in that area up to 1%. The cumulative effect of the smaller deviations may be determined with further study.

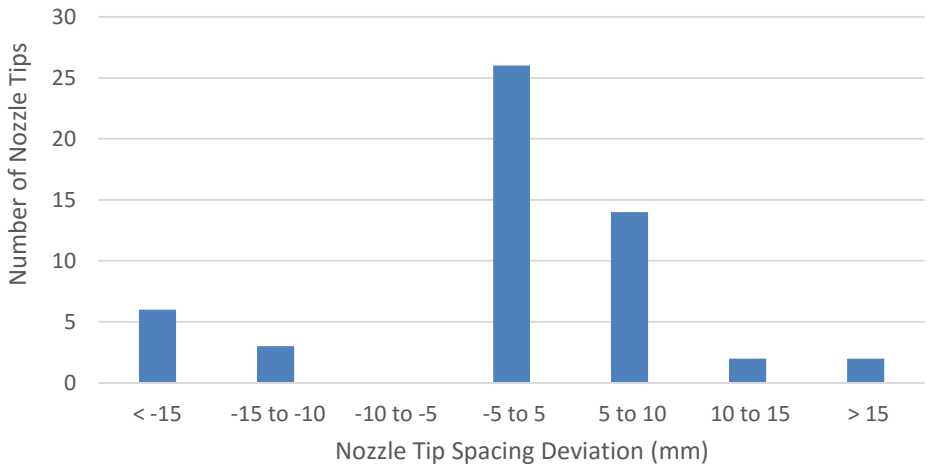

Figure 3.19: Number of nozzle tip spacings at various deviations (mm) from ideal spacing of 50.8 cm.

The data in Figure 3.19 summarize a similar analysis performed on the nozzle tip spacing measurements. While this information does not provide an absolute deviation (distance or angle) from vertical, it does provide insight into the nozzle to nozzle variation. For instance, six measurements between tips showed a spacing of less than 49.3 cm which indicates the nozzles were most likely angled towards each other. However, it would be possible to see situations where this might not be the case. One nozzle may be angled toward the right to such a degree that the next nozzle may be spaced closer than 50.8 cm even as it could be in a vertical or angled-to-the-right position. An analysis of the differences between nozzle body spacing and nozzle tip spacing indicates there may have been substantial errors with the lateral angles of nozzles. Assuming the lateral angle originated at the QJ360C nozzle body center rotation point (Figure 3.5), the nozzle tip spacing deviation and the distance from the center of rotation to the nozzle tip could be used to calculate the nozzle lateral angle. Based on a distance of 60 mm (center of nozzle body rotation to nozzle tip), a nozzle tip spacing deviation of 11 mm would result in a lateral angle change of 10°. The analysis of nozzle body spacing and nozzle tip spacing

provide evidence that multiple nozzles exceeded this angle. Considering the data contained in Table 3.1, this angle could have resulted in considerable errors across the boom. Assuming all lateral angles resulted from the nozzle body rotation may not hold true as some warped wet boom plumbing tubes may have contributed to deviations. The result of adding nozzle body and tip variations into the initial baseline simulation can be seen in Figure 3.20, referred to as the modified baseline simulation.

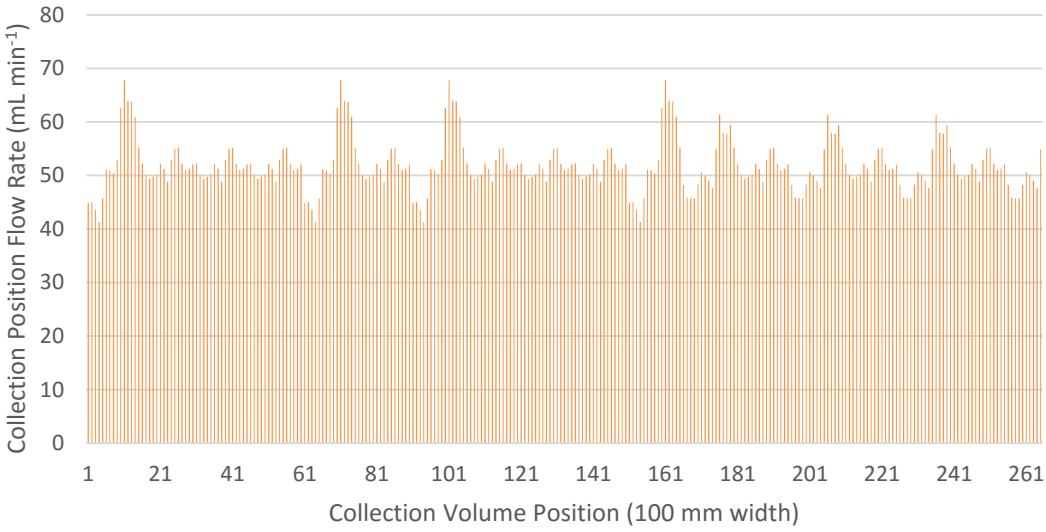

Figure 3.20: Modified baseline simulation of 27.4 m boom (100 mm collection widths) for the XR8003 laboratory nozzle data (CV 9.4%)

Using the laboratory data from the nozzle replacement tests (where an XR8001 and XR8005 were inserted in nozzle position #3, summarized in Table 3.3), two simulations were created by removing one section of baseline data contained in Figure 3.20, and replacing it with a set of data from a nozzle replacement test on the patternator in approximately the same location as nozzle #20 on the outdoor boom nozzle replacement tests. The resulting simulated boom distribution with an XR8001 nozzle is shown in Figure 3.21.

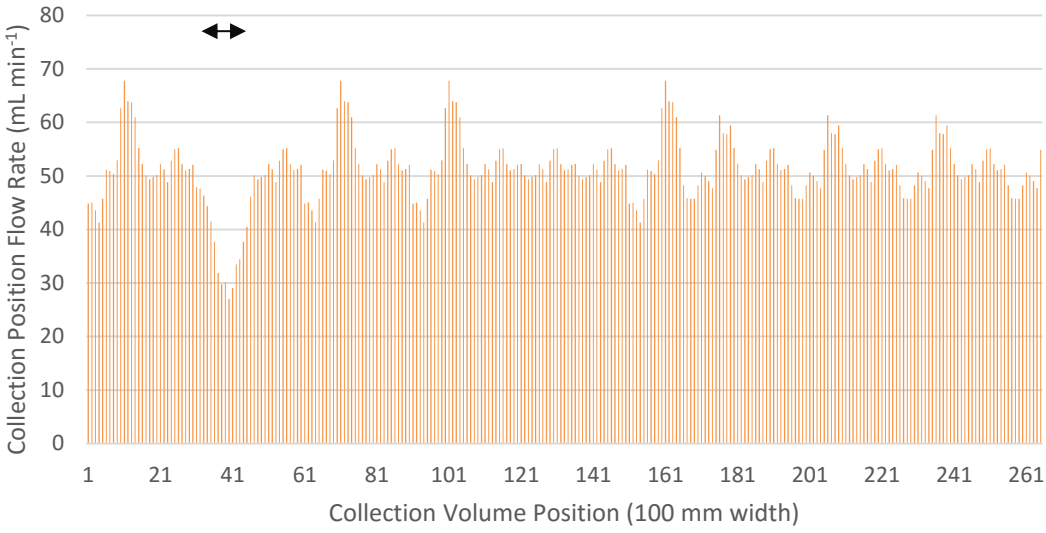

Figure 3.21: Simulated 27.4 m full boom scenario (CV 12.0%) created from patternator for XR8003 nozzles with one subsection of XR8001 spray pattern data inserted.

The full boom spray pattern distribution results from the Sprayertest 1000 with the one nozzle at position #20 replaced with an XR8001 nozzle is shown in Figure 3.22.

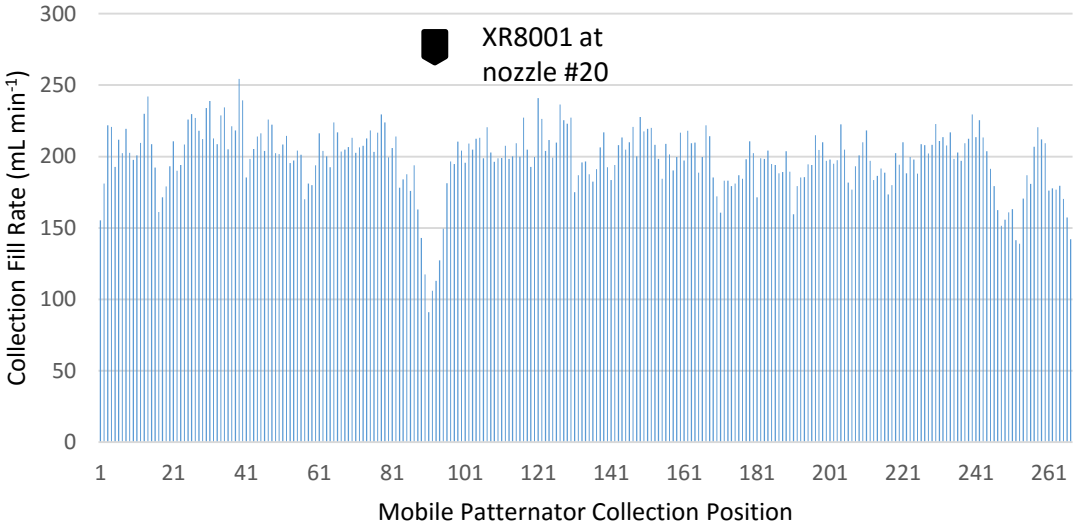

Figure 3.22: Spray pattern data from Sprayertest 1000 with XR8001 at nozzle at position #20.

A similar simulation was created using the laboratory spray pattern data for the XR8005 replacement test. The spray pattern data were averaged into 100 mm collection widths and one subsection (152 cm) with the XR8005 nozzle was substituted into the baseline

data set simulated in Figure 3.20. The resulting simulated boom distribution with the XR8005 nozzle is shown in Figure 3.23. The full boom spray pattern distribution results from the Sprayertest 1000 with one nozzle at nozzle #20 replaced with an XR8005 nozzle is shown in Figure 3.24.

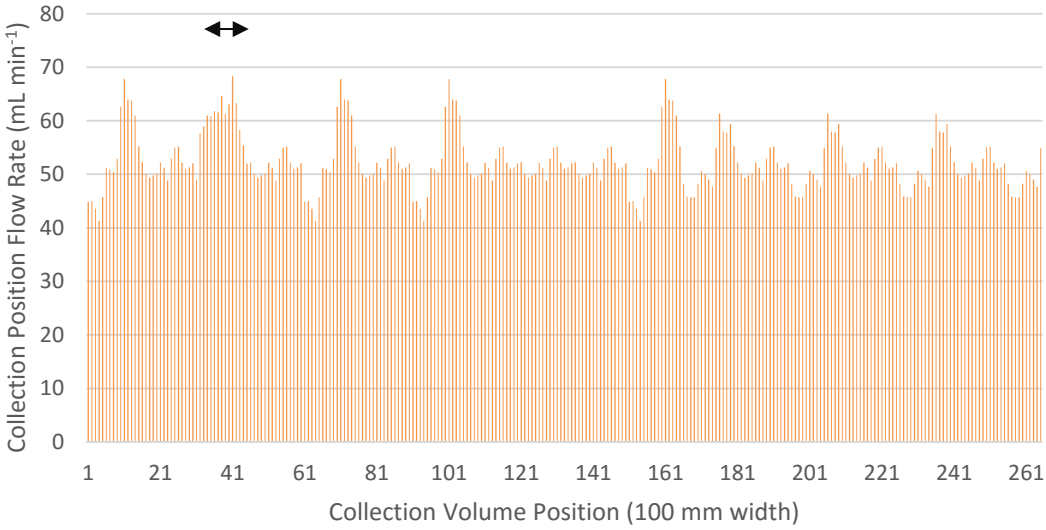

Figure 3.23: Simulated 27.4 m full boom scenario (CV 10.1%) created from patternator for XR8003 nozzles with one subsection of XR8005 spray pattern data inserted.

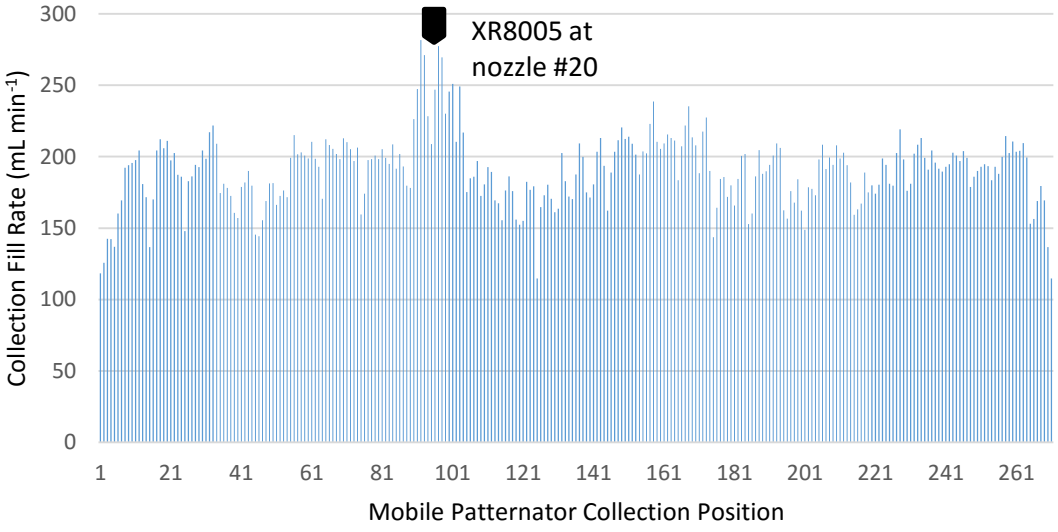

Figure 3.24: Spray pattern distribution data from Sprayertest 1000 with XR8005 at nozzle #20.

Table 3.7 summarizes the comparisons of the nozzle replacement tests from the Sprayertest 1000 with the simulations using data from the indoor patternator tests grouped into similar collection widths. While absolute CV values were different between the actual and simulated full boom tests, it was interesting to note the differences in CV from baseline within the actual and simulated tests were similar. The spray pattern CV in the simulation increased more than the spray pattern CV in the actual boom test for both nozzle replacements.

Table 3.7: Summary of comparison data between actual outdoor full boom tests with simulated data from indoor spray patternator nozzle replacement tests.

Test Setup	Average CV from Actual Full Boom Test (%)	CV Deviation from Baseline Actual Full Boom Test (%)	Average CV from Modified Simulated Full Boom Test (%)	CV Deviation from Baseline Simulated Full Boom Test (%)
Baseline	11.0	-	9.4	-
w/ XR 8001	13.3	2.3	12.0	2.6
w/ XR 8005	12.3	1.3	10.1	0.6

3.5 Conclusions

The nozzle lateral angle test showed a substantial increase in spray pattern CV at low angle changes for one of three nozzle spacings depending on the nozzle type. For any particular nozzle lateral angle for one of three nozzle spacings, the increase in spray pattern CV was larger for the 80° nozzles (XR8003 and XR8005) than for the 110° nozzles (XR11003 and AIXR11003). Spray pattern CVs exceeded 15% at nozzle lateral angles for one of three nozzle spacings for the XR8003 and XR8005 nozzles. The 110° nozzles did not experience CVs greater than 8.5% when the lateral angle was set to 8° for one of three nozzle spacings.

The nozzle spacing test showed that the spray pattern CV for the setups tested had a low sensitivity to spacing changes. For example the first 25 mm offset of the middleof three nozzle spacings with XR8003 nozzles resulted in a spray pattern CV increase of 0.9% and the second 25 mm offset (50 mm total) resulted in a total spray pattern CV increase of 2.4% relative to the initial test condition. Spray pattern CVs did not exceed 10% until the offset of the middle of three nozzle spacings was 125 mm, nearly one fourth of the original 51 cm nozzle spacing. Changes in CV were similar for both nozzles (80° and 110°) tested with respect to each spacing movement. The nozzle replacement test with the XR8003 nozzles had large flow rate changes with both the XR8001 and XR8005 nozzles, however, the spray pattern CV for three nozzle spacings increased 4.3% with the XR8005 nozzle as opposed to 14.8% with the XR8001 nozzle. Nozzle flow rates indicated much more of a change than CV in the nozzle replacement tests.

The nozzle pitch angle test had low sensitivity to pitch angle changes. The spray pattern CV remained below the 10% threshold of a good pattern even with 24° of rotation both in the fore and aft direction. In terms of boom setup, installing the wrong size nozzle has the most potential to affect spray boom uniformity. Although a wrong size nozzle may not affect CV past the acceptable threshold, flow rate could be drastically altered. A nozzle lateral angle error, especially with 80° nozzles, poses the second greatest risk to negatively affect spray pattern uniformity. Nozzle spacing errors may cause some decrease in spray pattern uniformity, however, the risk is much lower than the previously mentioned setup errors and nozzle fore and aft angle poses almost no risk of adversely affecting spray pattern uniformity.

Results from simulating full boom changes on laboratory based patternator data were a reasonable representation of the changes setup factors may have had on a full boom sprayer. The simulated full boom CVs were similar to the CVs of the full boom sprayer once the nozzle angle variation was accounted for and changes in CV due to one nozzle at nozzle #20 being replaced were very similar.

Chapter 4. Laboratory and Field-Based Investigation of Spray Boom Operational Variability and Measurement Effects on Flow, Pressure, and Pattern Distribution

4.1 Literature review

Agricultural equipment is used to apply fertilizers and pesticides to crops to foster growth and limit competition from weeds, insects and fungi. Application technology is constantly improving to ensure that the proper amount of chemical is applied to the target or area. Agricultural equipment have used electronic components since the mid 1960's, and most modern self-propelled equipment utilize embedded electronic control units [ECU] (Stone et al., 2008).

The most common ECU communication protocol is Controller Area Network (CAN) bus. CAN bus was first introduced by Robert Bosch GmbH (Bosch 1991) for automotive applications, however applications have expanded to marine, aviation, agriculture and forestry. The Society of Automotive Engineers (SAE) standard J1939 (SAE 2000) defines the format for CAN bus messages used in agriculture, among other heavy-duty applications. Early control systems were developed to adjust sprayer output to compensate for operation at speeds different from the speed at which the sprayer was calibrated (Gebhardt et al., 1974) based on wheel speed sensors or ground speed radars. Today, the majority of communication of operation parameters occurs on the CAN bus; little information is publicly available about the accuracy of these data.

Global positioning systems (GPS) have improved the ability of machinery to apply chemicals more precisely and allowed for the deployment of map-based automatic section control (ASC). Map-based ASC enables applicators to spray non-rectangular areas which before would have been either skipped or sprayed twice (Luck et al., 2010b)

and has been shown to decrease over-application from 12.4% to 6.2% when switched from five section manual control to seven section automatic control (Luck et al., 2010a).

Field efficiency is affected by field size, shape and equipment traffic patterns (Grisso et al., 2002). Turning in fields increase chances for overlap and off-rate application. In the (Grisso et al., 2004) study on field efficiency, a negative correlation was shown between steering angle and field efficiency during planting and harvesting. Loss of field efficiency due to turning would only increase on wider equipment such as sprayers. Commercially available turn compensation systems typically use pulse width modulation (PWM) of solenoid valves on boom subsections or individual nozzles to reduce application errors during turning. These systems have been shown to maintain nozzle flow rates within the documented ASABE standard (S592) of ±10% error (Porter et al., 2013; ASABE Standards 2011).

While boom section control and turn compensation systems improve spray application, (Luck et al., 2011a) found a majority of the fields in the study received rates below 90% of the target rate. The errors in rate were attributed to pressure variation from control system delays and turning movements (Luck et al., 2011a). (Sharda et al., 2010) found that nozzle tip pressures increased up to 20% when turning nozzle or boom sections off, resulting in a flow rate increase of 10.6%. The nozzle tip pressure increase was found to be proportional to the percent of boom sections turned off, and it was concluded that system flow rate did not represent tip flow rate during stabilization periods after section control changes (Sharda et al., 2010). When boom sections were automatically turned on or off during entry or exit of point rows, results showed over- and under-application during flow compensation tests (Sharda et al., 2011). Automatic section control (i.e.,

deliberate, automated flow control by the system) on boom subsections and individual nozzles have been evaluated (Sharda et al., 2013), but the effects of an obstructed hose or nozzle and potential error from pressure measurements along the boom have not. Non-uniform application due to pressure differences along the spray boom, compounded with indicated flow rates not consistent with nozzle output may be a limiting factor in proper chemical application and generation of as-applied maps. Figure 4.1 shows an as-applied map which was generated from section status, flow rate and GPS data. The map assumed even flow rate between all boom subsections. Application rates could be different across the boom, especially during settling times after an ASC event. Static tests on system flow rates, boom pressure and correlating spray pattern CV may improve future as-applied maps and reduce misapplication. (Sharda et al., 2013) stated that static testing can give a reasonable estimate of how the sprayer will perform in the field.

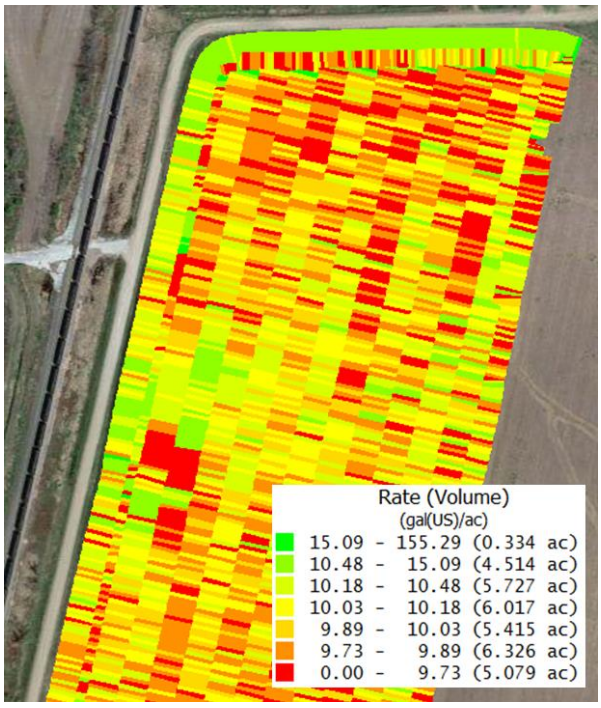

Figure 4.1: Typical as-applied map generated from sprayer section status, flow rate and GPS data.

4.2 Goals and objectives

The goals of this project were to obtain information regarding the relationship among nozzle flow rates, system flow rates, system pressure and spray pattern distribution and the potential errors associated with the system measurements for estimating the spray boom distribution. The objectives of this project were to 1) evaluate operational factors and their effect on spray pattern uniformity and determine how full boom simulations from lab data compare to full boom sprayer testing, 2) determine relationship among nozzle flow rate, pressure and full boom spray pattern uniformity, and 3) determine relationships between errors in system flow rate and pressure measurements, and potential errors across the width of a spray boom.

4.3 Materials and Methods

Spray pattern distribution data, system pressure and nozzle flow rates were recorded using an automated laboratory spray patternator as outlined by (Luck et al., 2016). The patternator collected 152 cm sets of spray pattern distribution data in 25 mm collection widths, as well as pressure data. The spray pattern collection system used signals from liquid-level sensors to record the time to fill a fixed-volume container in a virtual instrument (VI) in LabVIEW (National Instruments 2014). The time and volume data were converted into a flow rate (mL min^{-1}) for each 25 mm collection width. Boom and nozzle pressure data were collected using electronic pressure transducers (Omega Engineering PX309-100G5V) plumbed into the spray boom or a tee mounted on the nozzle body. The VI exported an Excel file with the time to fill each container and the average pressure from each pressure transducer at the conclusion of each test. Coefficient of variation (CV) was used as a measure of dispersion among the flow rates for the

collection widths to evaluate the uniformity of the spray pattern distribution. CV was also used to quantify the dispersion among nozzle flow rates. CV is defined as the sample standard deviation divided by the mean of a data set as outlined in Equation 4.1.

$$CV(\%) = (100\%) \cdot \sqrt{\frac{\sum_{i=1}^{n}(x_i - \bar{x})^2}{n-1}} \Bigg/ \frac{\sum_{i=1}^{n} x_i}{n} \qquad \text{Equation 4.1}$$

4.3.1 Laboratory Data

A nozzle obstruction test was set up with six XR8003 (TeeJet Technologies, Wheaton, Ill.) nozzles placed 76 cm above the patternator in 51 cm spacings. The third (from left) nozzle was selected as the treatment nozzle and was fitted with a valve to simulate an obstruction or blockage in the line or nozzle body (Figure 4.2). Starting with 100% flow, measured in ($mL \cdot min^{-1}$), the valve was used to reduce flow in approximately 5% increments, down to 45%. At each valve setting the spray pattern distribution, nozzle flow rates and nozzle pressure were recorded with the system pressure set to 207 kPa. This procedure was conducted both with the pressure transducer upstream and downstream of the obstruction valve to determine if pressure changes could be detected along the boom from the pressure measurements.

The test was repeated with AIXR11003 nozzles with a system pressure of 345 kPa. Nozzle pressure CV and spray pattern CV were plotted against nozzle flow rate to show the rate of CV increase with each 5% decrease in flow rate. Test results were analyzed for significant differences using a general mixed model (GLIMMIX) in SAS v9.4 (SAS Institute Inc. 2013). A least significant means (LSM) test with an alpha if 0.05 was used

to determine which treatments produced significantly different spray pattern and nozzle flow rate CVs.

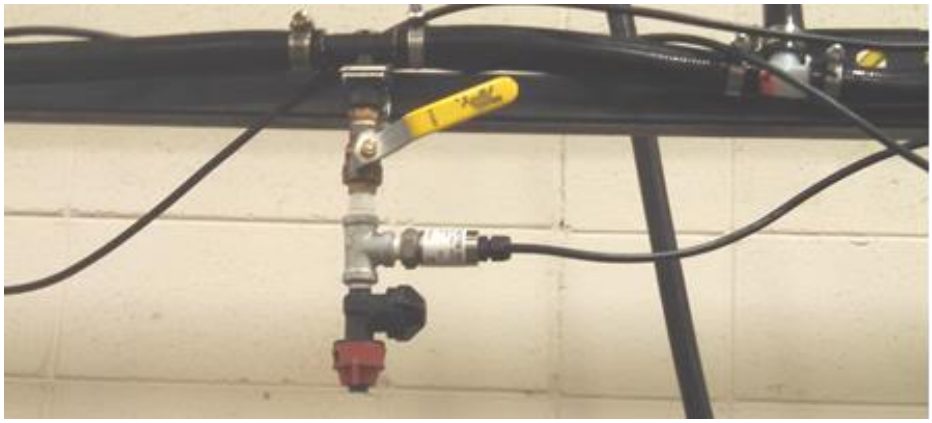

Figure 4.2. Nozzle obstruction device on nozzle #3 with pressure transducer downstream of obstruction.

4.3.2 Comparisons of Lab Data vs. Full Boom Pattern Uniformity

Full boom simulations were created using 152 cm sets of 25 mm collection width spray pattern data averaged into 100 mm collection width. The spray pattern data from the patternator (in 25 mm increments) were averaged into 100 mm collection widths for direct comparison with the data from a full boom sprayer, which was measured in 100 mm increments. A baseline simulation was created by extrapolating pattern data from the patternator with no flow obstructions out to a width of 27.4 m. One 152 cm portion was then replaced with three 51 cm sets from the center nozzle of the nozzle obstruction test to estimate the CV of a full boom sprayer with a similar obstruction and compare with full boom sprayer testing. During all three reps of one obstruction test, 3 of the six nozzles on the sprayer produced zero flow. Of the nozzles the produced zero flow, two nozzles were consecutive and one zero flow nozzle with nozzles producing flow on either side of it. To compensate for this in the simulation three 51 cm subsection widths were

changed to zero flow and placed in the simulation in similar placement as the nozzles producing zero flow on the full boom sprayer.

An Apache AS1020 self-propelled sprayer with 54 XRC8003 nozzles was instrumented with ten electronic pressure transducers (Omega Engineering PX309-100G5V) installed inline within the boom supply hoses to record boom subsection pressure. The pressure transducers had an operating range of 0 to 690 kPa correlating to a 0 to 5 V DC signal. The output signals were record by a microcontroller (Arduino Mega 2560, Arduino LLC, Ivrea, Italy) sampling at 1 Hz, and output to a comma delineated .txt file. A manual pressure gauge (Figure 4.3), with a minimum increment of 6.9 kPa (1 psi), mounted to a nozzle body was used to monitor nozzle pressure of each individual nozzle, once during each test (PGS-35L-100, Omegadyne, Inc., Sunbury, Ohio).

Figure 4.3: Manual pressure gauge for monitoring nozzle pressure.

A flow limiting valve was placed on the supply line to the #4 boom subsection (from left) ahead of the pressure transducer. Figure 4.4 shows the locations of the pressure transducers and the flow limiting device with respect to the boom subsections. Three replicates of nozzle flow rate for each nozzle were recorded using a 250 ml graduated cylinder with graduations in 2 mL increments, and a stopwatch.

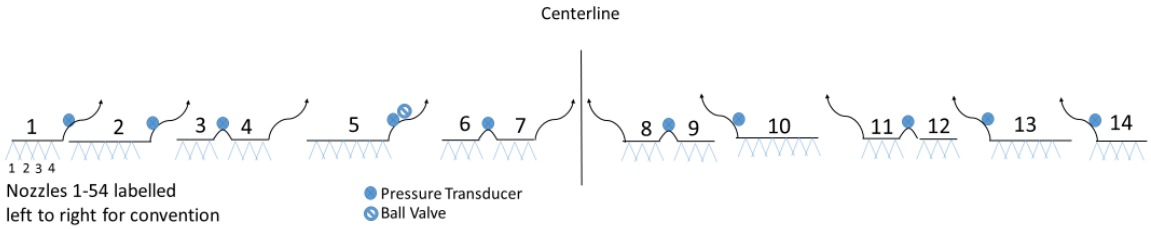

Figure 4.4: Boom diagram of Apache AS1020 sprayer showing locations of pressure transducers and flow limiting valve.

A mobile outdoor patternator (Sprayertest 1000, Herbst pflanzenschutztechnik, Hirschbach, Germany), was used to collect spray pattern data from the AS1020 sprayer. The Sprayertest 1000 was an automated cart which travelled on a track placed under the boom by the operator. The cart used ten 100 mm collection troughs to collect spray pattern data, recording the spray pattern 1 m at a time. Companion software to the Sprayertest 1000 was used to set the location of the first and last nozzle, start or stop measurements, and output the spray pattern data once a test had concluded.

Figure 4.5: Herbst Sprayertest 1000 mobile patternator used for measuring full boom pattern distributions.

Once the first and last nozzle positions were set, the cart would move to the centerline of the first nozzle, record a pattern measurement then move one table width toward the last nozzle, and repeat this process until the entire boom pattern was measured. The Sprayertest 1000 was set up to record spray pattern measurements from the centerline of the first nozzle to the centerline of the last to ensure the entire spray pattern was collected. Data were post processed to remove spray pattern measurements with inadequate nozzle spray overlap.

To test the effect of a flow obstruction on spray pattern a ball valve was plumbed in before the #4 (from left) boom subsection and set at two positions by partially closing the valve. The first position obstructed the pressure to the fourth boom section to approximately 77% of the baseline flow rate, the second setting restricted pressure to approximately 56% of the baseline flow rate. These flow rate restrictions corresponded to 60% and 33% of system pressure (207 kPa), repectivley. Three replicates of pattern data were collected for both 77% and 56% restriction settings along with nozzle flow rate, nozzle pressure, and boom section pressure data.

4.3.3 Full Boom Pressure, Flow and System Based Estimates

A data acquisition system was created to simultaneously record CAN bus and system pressure data on a different Apache sprayer (AS715, Equipment Technologies, Inc., Mooresville, IN, USA). The sprayer was equipped with a Raven SCS 500 rate controller (SCS500, Raven Industries, Inc., Sioux Falls, SD) and the boom was fitted with XRC8003 (54 total) nozzles. A virtual instrument (VI) was created in LabVIEW which collected data from a National Instruments cDAQ-9174 four slot DAQ with NI 9862

High speed CAN and 9205 analog input modules to record the data from the sprayer (Figure 4.6).

Figure 4.6: National Instruments cDAQ with 9205 analog input module and 9862 high-speed CAN module used to collect pressure and flow rate data.

Analog data were collected from eight pressure transducers (Omegadyne PX309-100G5V, Stamford, CT) plumbed into the boom subsections and boom supply lines (Figure 4.8). The VI operating the hardware used a waveform chart to display the data in real time and logged the data to a .TDMS file for post processing.

The SAE-based CAN bus format is structured into seven layers based on the ISO 7498 Open System Interconnect (OSI) model (SAE 2000). The standard allows for use of either the “standard” 11 bit identifier or an “extended” 29 bit identifier. SAE J1939 and ISO 11783 use similar message structure, this allows multiple Electronic Control Modules (ECU) to be connected and transmit or receive data on the bus. While some messages are defined by standards, many of the messages used in agricultural equipment are proprietary. The messages are identified by a Parameter Group Number (PGN) to uniquely identify messages so ECUs can accept or ignore the data passed by each

message. Message data are passed in American Standard Code for Information Interchange (ASCII) format. A wiring harness (Figure 4.7) was built to read messages between the CAN bus on the sprayer and the Raven rate controller in the cab.

Figure 4.7: Wiring harness for reading messages from CAN bus between a sprayer and rate controller.

To decode proprietary messages, bits of hexadecimal data were manually converted to decimal form. The converted decimal data were verified against the values displayed on the Raven SCS5000 monitor. Once the raw data was matched to values on the monitor, the bit position and length of the desired data were confirmed. Once the start bit and length of the desired messages were confirmed, a database file was made for the LabVIEW VI to collect the messages.

To evaluate the effect of a blocked boom section or hose a ball valve was placed before boom subsections three and four (from left) in the supply line. To test the effect of a blockage, four ball valve settings were used: full flow with the ball valve fully open, zero flow with the ball valve completely shut, and two intermediate settings (95% and 80% of full flow). To determine the flow rate percentage, the average of the obstructed boom

section flow rates were divided by the average of the unobstructed boom section flow rates. Figure 4.8 illustrates the spray boom with the locations of the ball valve and the pressure transducers.

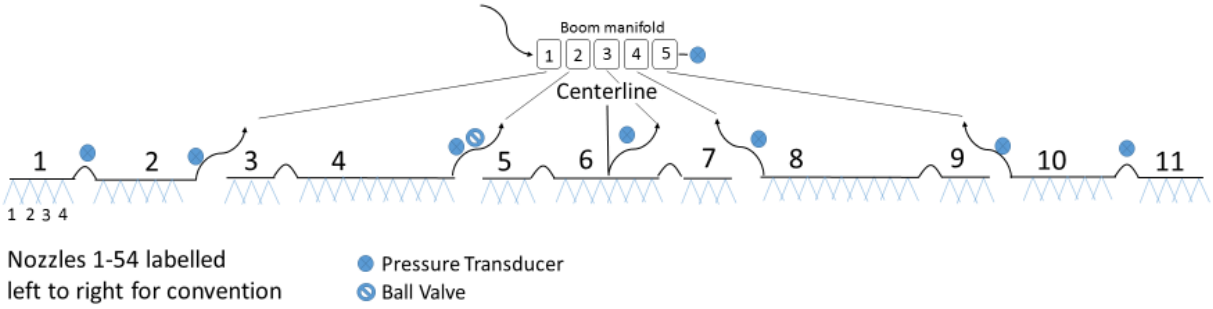

Figure 4.8: Diagram of boom plumbing system of Apache AS715 with locations of electronic pressure sensor and ball valve.

At each flow restriction setting, data at four pressure settings: 207 kPa, 275 kPa, 345 kPa, 414 kPa were recorded for a total of 16 flow obstruction and pressure setting combinations. For each pressure setting and flow restriction combination the product pump on the sprayer was turned on and allowed to reach steady state. Once steady state was achieved, nozzle flow rates were recorded from one nozzle (selected randomly each time) within each boom subsection (for a total of 11 flow rate measurements) with a graduated cylinder with a minimum increment of 5 ml and a stop watch, while the CAN bus-indicated system flow rate and analog pressure transducer data were recorded continuously on the DAQ. Once steady state was reached 5 min of pressure and flow data were post-processed for analysis. To compare the effects of an obstruction on the nozzle flow rates, individual nozzle flow rates were estimated from Equation 4.2, which was calculated from the orifice outputs for the nozzle (TeeJet Technologies 2015)

$$\text{Nozzle Flow (L min}^{-1}\text{)} = 0.0023*(\text{Pressure kPa}) + 0.4749 \qquad \text{Equation 4.2}$$

Boom subsection pressures and the number of nozzles in the corresponding subsection were used to estimate flow rates output from each boom subsection. Another sprayer flow rate was calculated based on the system pressure and the total number of nozzles to estimate the flow rate a pressure based system might have predicted. System flow rates were compared between the CAN bus-indicated flow rate and hand measured flow rate, system pressure calculated flow rate, and boom subsection pressure calculated flow rates. A total of four flow rates were used for comparison. Flow rates based on pressure were calculated using Equation 4.2. The CAN bus-indicated flow rate was taken to be the reference flow rate in the percent difference comparison calculations. Percent difference between the flow rates was calculated by taking the difference between the CAN bus-indicated flow rate and the flow rate being compared, divided by the CAN bus indicated flow rate. Flow rates of each boom subsection were compared by dividing the CAN bus indicated flow rate by the proportion of nozzles in each boom section, compared to nozzle flow rate measurements multiplied by the number of nozzles in each boom subsection. The percent difference was calculated in a similar manner as the system flow rate percent differences were calculated.

4.4 Results and Discussion

4.4.1 Laboratory Data

The results from the nozzle obstruction test with the obstruction downstream of the pressure sensor at nozzle position #3 are summarized in Table 4.1. The average flow rate from the 3 replicates for the test nozzle (third from left) is shown in percent of full-flow rate and total flow rate along with nozzle flow rate CV (for six nozzles), average spray pattern CV, and average boom pressure. Nozzle flow rate CV changed more (1.5% to

21.4%) than pattern CV (4.7% to 16.1%) as the obstruction increased, suggesting a nozzle flow rate CV measurement could provide easier detection of obstructions than other indicators. The pressure drop at the obstructed nozzle was not detectable in other areas of the boom. As the obstructed nozzle flow rate reduced from 100% to 91%, the nozzle flow rate CV increased from 1.5% to 3.4%, while the spray pattern CV increased from 4.7% to 6.0%. These changes indicate a relatively small increase in both nozzle flow rate and spray pattern CV. As the flow was reduced from 63% to 51% of full flow, the nozzle flow rate CV increased from 15.7% to 20.4%, while the spray pattern CV increased from 8.1% to 13.0%. At the point in which the spray pattern CV crossed the threshold of 10% (maximum pattern CV considered desirable), the obstructed nozzle flow rate had dropped to nearly half the full flow rate. Spray pattern CV test could report an acceptable spray pattern even though the flow rate through one out of three nozzles is obstructed to 60% of its full flow rate. It should be noted that pressure changes due to the obstruction were not detectable elsewhere in the boom during the obstruction test.

Table 4.1. Summary of XR8003 nozzle obstruction test (obstruction downstream of pressure transducer) comparing nozzle #3 flow rate, nozzle flow rate CV and spray pattern CV.

Nozzle #3 Flow Rate (% of full flow rate)	Average Nozzle #3 Flow Rate ($mL \cdot s^{-1}$)	Mean CV† of 6 Nozzle Flow Rate Values (%)	Mean† (of 3 replicates) Spray Pattern CV (%)	Average Boom Pressure (kPa)
100	16.7	1.5[a]	4.7[a]	205.6
94	15.7	2.6[b]	5.6[b]	208.3
91	15.3	3.4[c]	6.0[c]	206.3
84	14.0	6.5[d]	6.4[d]	204.9
80	13.4	7.9[e]	7.3[e]	207.6
73	12.1	11.3[f]	7.4[e,f]	205.6
70	11.8	12.5[g]	7.7[f]	208.3
63	10.5	15.7[h]	8.1[g]	207.0
60	10.0	17.2[i]	9.3[h]	207.6
51	8.6	20.4[j]	13.0[i]	205.6
45	7.6	21.4[k]	16.1[j]	207.0

†Mean CVs with same letter are not significantly different ($p \leq 0.05$). Nozzle flow rate CVs with same letter are not significantly different ($p \leq 0.05$).

Table 4.2 summarizes results from the nozzle obstruction test when the obstruction was upstream of the nozzle #3 pressure transducer. As the obstruction of nozzle #3 increased, both the nozzle flow rate and spray pattern CVs increased. The decrease in pressure at nozzle #3 caused by the obstruction can be observed by comparing the nozzle 1 and 2 pressures with the nozzle 3 pressure. As the flow rate to nozzle #3 was reduced, the pressure at the nozzle also decreased, as reflected in the nozzle #3 pressure column of Table 4.2. The spray pattern CVs at 94%, 86% and 77% of full flow were not significantly different (Table 4.2), though nozzle flow rate CVs at those settings increased significantly. The spray pattern CV would have been considered in the desirable range (CV < 10%) for flow rates to nozzle #3 between 100% and 77% of full flow. It should be noted that boom pressure did not indicate the obstruction and did not reflect the changes in obstruction.

Table 4.2. Summary of XR8003 nozzle obstruction test results (obstruction device upstream of pressure transducer) with nozzle #3 flow rates, nozzle pressures, and spray pattern CVs.

Nozzle #3 Flow Rate (% of full flow rate)	CV† of 6 Nozzle Flow Rate Values (%)	Nozzle 1 Pressure (kPa)	Nozzle 2 Pressure (kPa)	Nozzle 3 Pressure (kPa)	Nozzle 3 Pressure (% of full pressure)	Mean† (of 3) Spray Pattern CV (%)
100	1.5[a]	202.7	207.4	204.7	100.0	4.0[a]
94	2.9[b]	205.3	209.5	182.3	89.0	5.9[b]
86	6.4[c]	205.3	209.4	149.0	72.8	5.7[b]
77	10.2[d]	198.0	200.2	123.9	60.5	6.6[b]
66	14.8[e]	202.3	206.9	82.2	40.1	11.0[c]
56	19.4[f]	204.0	208.7	63.5	31.0	12.4[d]
44	25.0[g]	205.2	210.0	57.2	27.6	18.0[e]

†Mean CVs with same letter are not significantly different ($p \leq 0.05$).

Figure 4.9 illustrates the spray pattern CV and test nozzle pressure data as the test nozzle flow rates were reduced. Changes in pressure at nozzle #3 were evident in Table 4.2 as

the flow decreased due to the location of the pressure sensor. Spray pattern CVs increased as flow from nozzle #3 was reduced but were not as prominent as changes in nozzle flow or pressure.

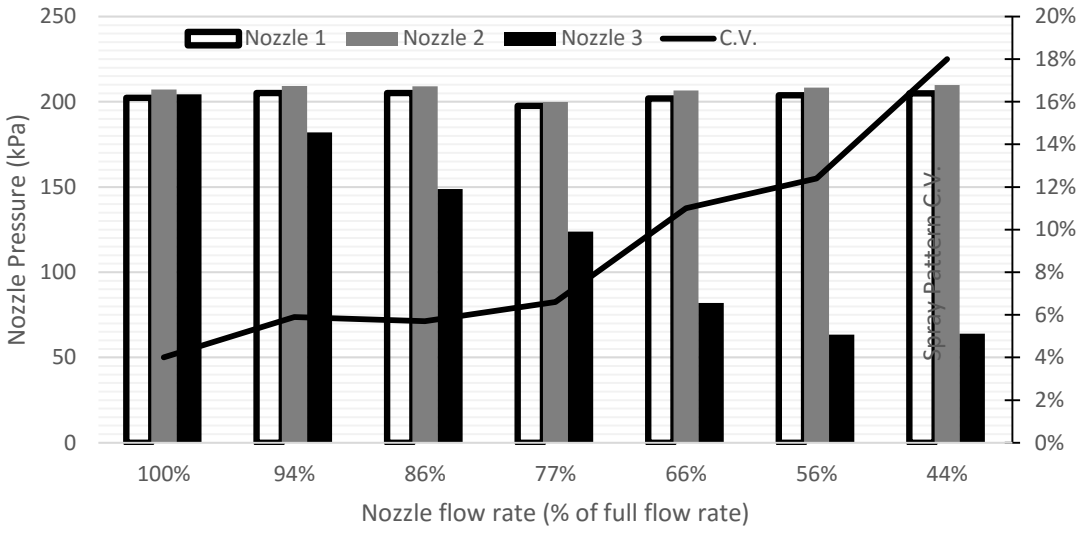

Figure 4.9: Nozzle pressire and spray pattern CV plotted against flow rate of three nozzles (XR8003) in the nozzle obstruction test as the flow rate through test nozzle (nozzle #3) was reduced from 100% to 44% of full flow.

The obstruction test was repeated with AIXR11003 nozzles with the results summarized in Table 4.3. The data from Table 4.3 are shown graphically in Figure 4.10. As the flow through nozzle #3 was decreased, the spray pattern CV increased. AIXR nozzles showed changes in spray pattern CV and nozzle flow rate CV similar to the XR8003 nozzles. These findings suggest that AIXR and XR nozzles are affected by obstructions in a similar manner and performance deteriorates similarly for both. An obstruction in a boom impacts the nozzle flow rate CV more so than the spray pattern CV.

Table 4.3. Summary of nozzle obstruction results with nozzle #3 flow rates, nozzle pressures, and spray pattern CVs. All nozzles were AIXR11003.

Nozzle #3 Flow Rate (% of flow rate)	CV of (6) Nozzle Flow Rate Values (%)	Nozzle 1 Pressure (kPa)	Nozzle 2 Pressure (kPa)	Nozzle 3 Pressure (kPa)	Average (of 3 replicates) Spray Pattern CV (%)
100%	1.6	337.2	337.0	340.1	4.9
95%	3.4	340.0	340.0	311.1	5.3
90%	5.7	343.1	343.0	277.6	5.9
86%	7.2	342.4	342.1	251.0	6.5
79%	10.4	343.7	343.8	207.0	8.1
74%	12.3	343.3	343.3	183.6	9.4
71%	13.7	343.0	342.7	166.8	10.4
66%	16.0	343.4	343.5	144.6	11.7
60%	18.7	341.6	341.5	117.3	13.9
56%	20.6	343.5	343.2	100.2	15.2
50%	23.4	347.2	346.6	81.9	17.8
47%	24.8	347.6	347.2	69.7	19.9

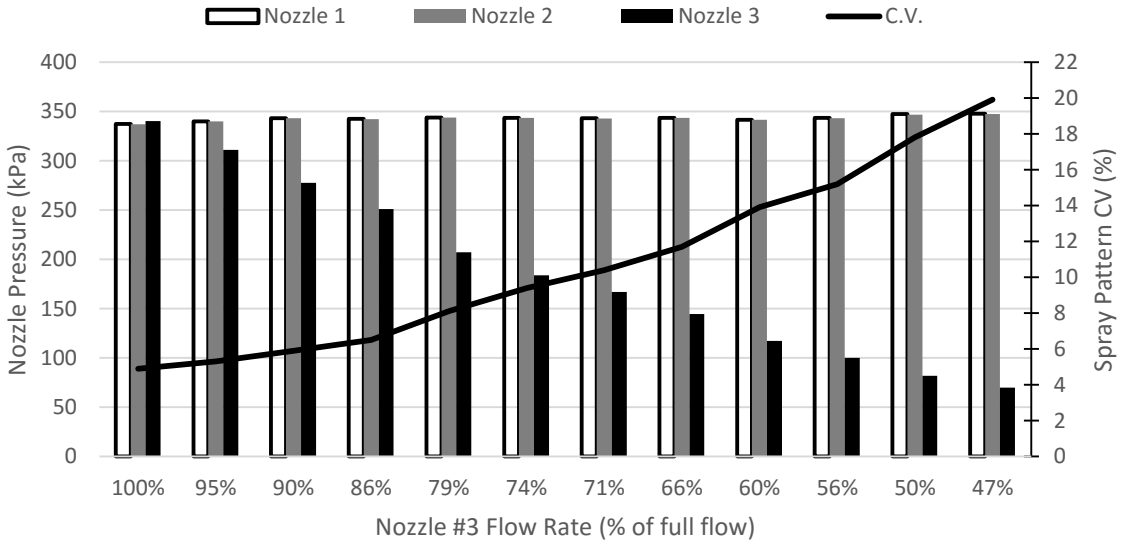

Figure 4.10: Nozzle pressure and spray pattern CV at each nozzle flow rate setting as the flow through nozzle #3 was reduced from 100% to 47% of full flow during nozzle obstruction test (AIXR11003).

4.4.2 Comparison of Laboratory Simulated Pattern Data versus Full Boom Field Pattern Test

To determine the effect of collection width on CV, 25 mm collection data were averaged into 100 mm collection and CV values compared. Figure 4.11 illustrates the effect of the 25 mm collection width data averaged into 100 mm collection widths from the first obstruction tests (Table 4.1). This was done so data from the patternator could be compared to spray pattern data from a full boom sprayer, which was measured in 100 mm collection widths. Figure 4.11 shows the CV values of the nozzle obstruction test both in the original 25 mm collection width and after conversion to 100 mm collection width. As shown in Table 4.4 the CV of each data set was reduced by almost 0.5% (e.g. at 100% flow rate for nozzle #3, the CV was reduced from 4.7% to 4.3%). This result is most likely a change due to data smoothing as CV is a measure of dispersion averaging groups of data points results in data sets with less variation, resulting in the lower CVs for the 100 mm collection width data sets. A baseline simulation spray pattern was created using lateral angle test results corresponding to rotation angles measured from nozzle body and tip spacings.

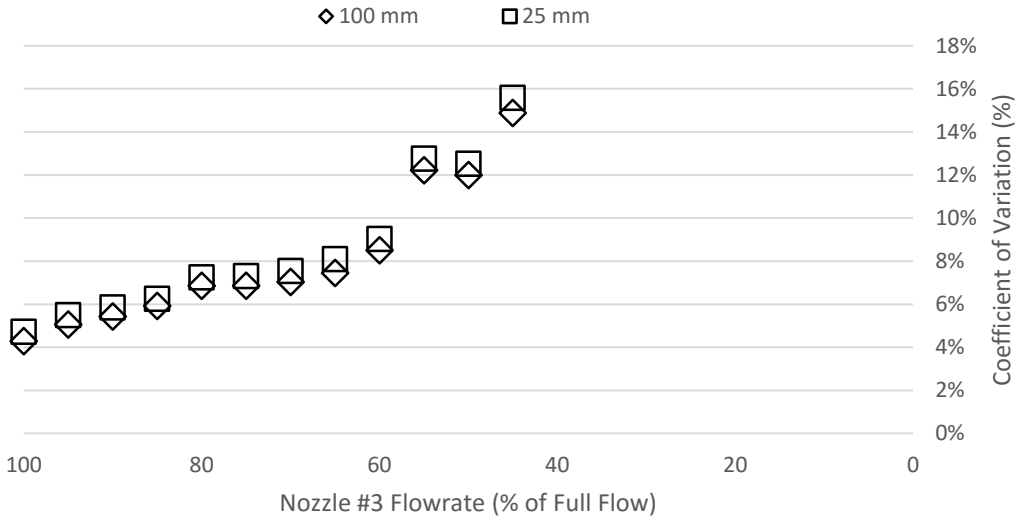

Figure 4.11: Twenty five mm collection width and 100 mm collection width spray pattern CVs with XR8003.

Table 4.4: XR8003 spray pattern (152 cm width) CV data grouped by different collection volume widths.

Nozzle #3 Flow Rate (% of open fully open valve)	Spray Pattern CV for 100 mm collection widths (%)	Spray Pattern CV for 25 mm collection widths (%)
100%	4.3%	4.7%
94%	5.1%	5.6%
91%	5.5%	6.0%
84%	6.1%	6.4%
80%	7.0%	7.3%
73%	6.9%	7.4%
70%	7.1%	7.7%
63%	7.8%	8.1%
60%	8.7%	9.3%
51%	12.5%	13.0%
45%	15.4%	16.1%

Simulations were created to model a boom obstruction and compare with the outdoor boom section flow obstruction test. Spray pattern data from the laboratory nozzle flow obstruction tests (summarized in Table 4.2) were averaged into 100 mm widths across the 152 cm patternator width. Two sets of laboratory test data were chosen that most closely

represented the outdoor test results in terms of boom section pressure after the valve was closed. The laboratory test data included the spray patterns for nozzle #3 with flow rates at 77% (corresponding to a boom section pressure of 60%) and 56% (corresponding to a boom section pressure of 33%) to compare with the outdoor scenarios. The center 51 cm of both laboratory spray pattern data were repeated six times as the outdoor boom section flow reduction tests affected six consecutive nozzles in boom section #4. These data created a simulated boom section with six nozzles at approximately the same pressure reduction as the outdoor test. The first simulation included the data for estimating the full boom spray pattern CV when the boom section was at 77% of full flow rate and is shown in Figure 4.12. This simulation boom section was developed for comparison with the data shown in Figure 4.13.

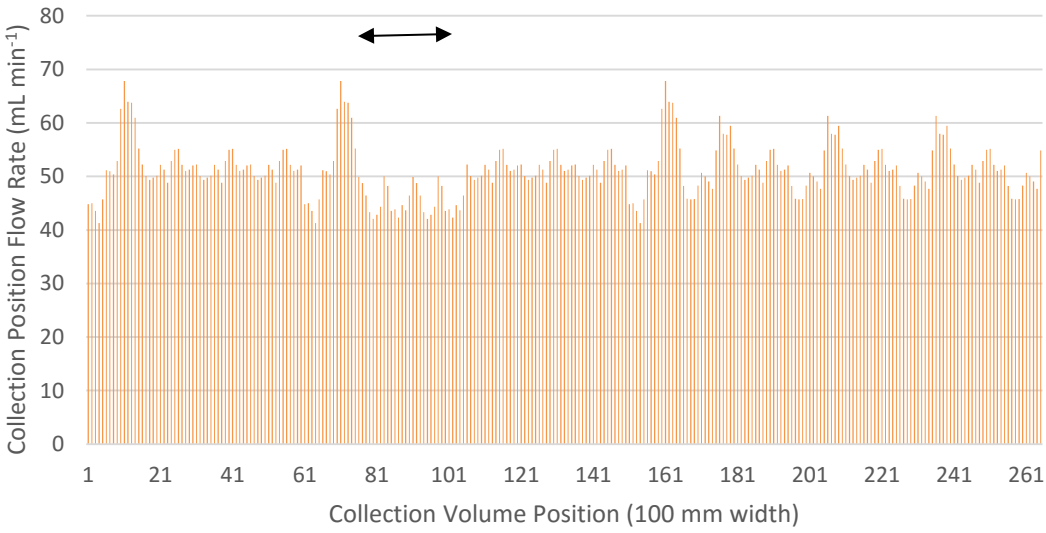

Figure 4.12: Simulated 27.4 m full boom scenario (CV 9.7%) created from patternator for XR8003 nozzles with a subsection (six nozzles) operating at approximately 77% of full flow rate.

The CV of the simulation was 9.7% while the full boom pattern CV was 14.3%. The initial CV changes values were quite different but the effects on CV from the obstruction were the object of the comparison.

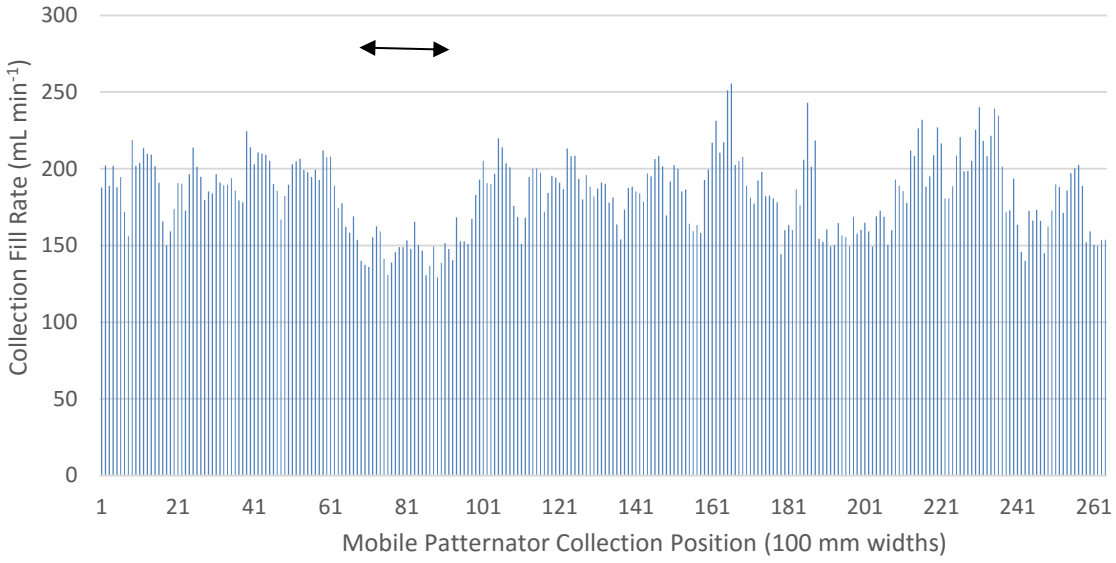

Figure 4.13: Mobile spray patternator CV data for 77% of full flow rate for boom section #4.

Figure 4.14 represents the full boom simulation when the patternator data were used to estimate the effects of having six nozzles at 56% of full flow rate. The resulting average spray pattern CV for the simulated entire boom was 8.3%. The data in Figure 4.14 was intended for comparison with Figure 4.15. During the actual outdoor test, three of the six boom section nozzles had zero flow which was not expected. There may have been some discrepancy in the check valve pressure at those nozzle bodies which may have caused those check valves to remain closed. Therefore, the CV from the simulation was much lower than that of the actual test. To evaluate the effects of the three nozzles with zero flow using simulated data, three 51 cm subsection widths from the data in Figure 4.14 were changed to zero. Two of the nozzles with zero flow were consecutive. The simulated boom was set up to reflect this. This created a full boom simulation which more closely matched the actual outcome from the outdoor test with the boom section at 56% of full flow rate. The resulting full boom simulation is shown in Figure 4.16 and would be comparable to the outcome of outdoor testing in Figure 4.15.

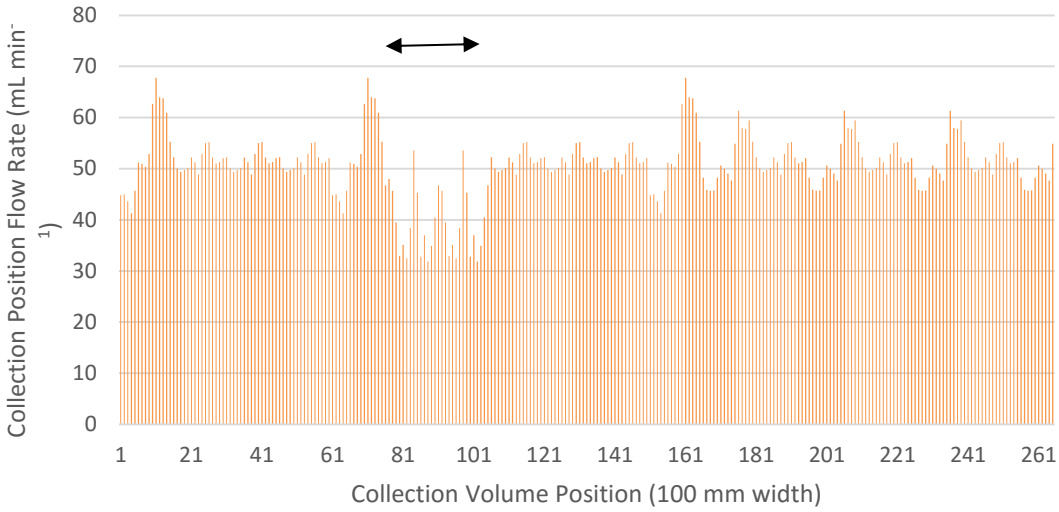

Figure 4.14: Simulated 27.4 m full boom scenario (CV 12.4%) created from patternator for XR8003 nozzles with a subsection (six nozzles) operating at approximately 56% of full flow.

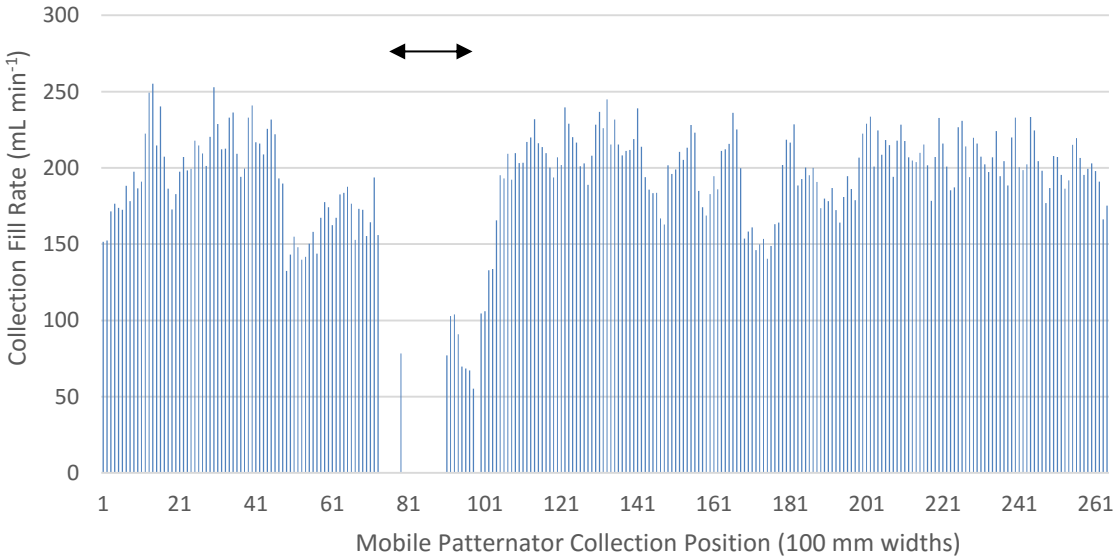

Figure 4.15: Mobile spray patternator CV data with boom section #4 at 56% of full flow rate.

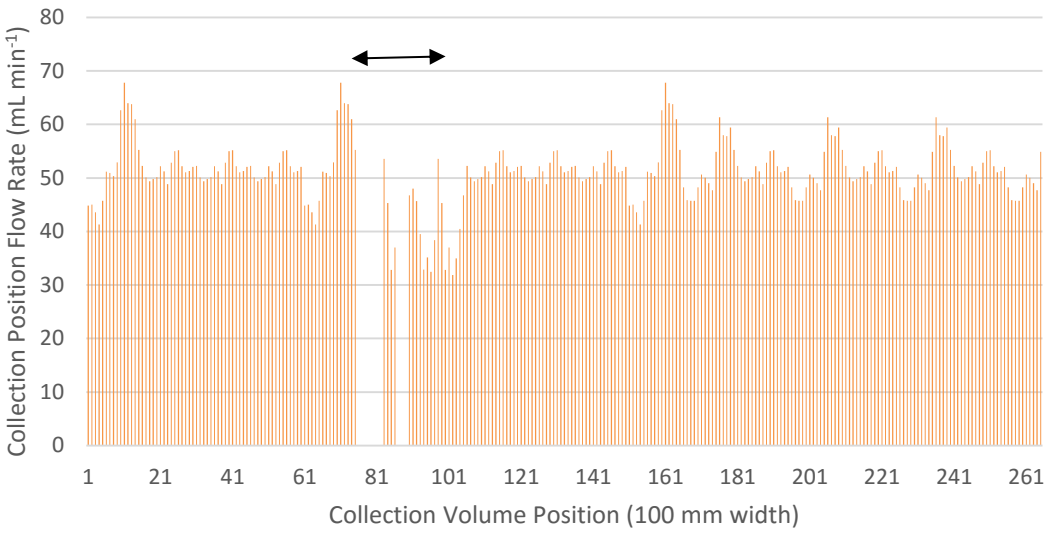

Figure 4.16: Simulated 27.4 m of full boom scenario (CV 22.8%) created from patternator for XR8003 nozzles with a subsection at approximately 56% of full flow rate and three nozzles with zero flow.

The comparison between data from the actual outdoor testing and simulating similar treatments using the indoor patternator tests are summarized in Table 4.5. With the variation due to nozzle body and tip spacing accounted for, the spray pattern CVs were comparable. When the simulated boom section pressure was reduced to 77% of full flow rate, the simulated data predicted a 0.3% increase in CV while the actual data increased 3.3% during outdoor tests. The second simulation yielded poor results, comparison between simulated versus actual CVs when the boom section flow rate was reduced to 56% differed greatly, at 3.0% and 20.6% increases in from baseline CVs, respectively. However, during the outdoor tests, three nozzles were found to produce zero flow within the restricted boom subsection. When these data were accounted for in the simulation, the changes in CV from baseline data were more comparable for the simulated (13.4%) and actual (20.6%) tests.

Table 4.5: Summary of comparison data between actual outdoor full boom tests with simulated data from indoor spray patternator of nozzle restriction test.

Test Setup (Boom Section #4)	Average CV from Actual Full Boom Test (%)	CV Deviation from Baseline Actual Full Boom Test (%)	Average CV from Modified Simulated Full Boom Test (%)	CV Deviation from Baseline Simulated Full Boom Test (%)
Baseline	11.0	-	9.4	-
at 60% pressure	14.3	3.3	9.7	0.3
at 33% pressure	-	-	12.4	3.0
at 33% pressure w/ no flow at 3 nozzles	31.6*	20.6*	22.8	13.4

*as previously mentioned, the outdoor testing with actual full boom with boom section #4 at 33% operating pressure resulted in 3 (of six total) nozzles within that section having no flow.

The first ball valve setting resulted in a restricted pressure of approximately 60% of the system pressure, which resulted in approximately 75% of full flow for the six nozzles in the restricted boom section. As shown in Table 4.6 the decreased flow from the six nozzles in the boom section #4 increased the full boom pattern CV by 3.3% while the CV for the nozzle and boom section pressures and flow rates increased substantially.

Table 4.6: Summary of spray pattern, nozzle pressure, boom section pressure and nozzle flow rate CV data for boom section #4 flow restriction tests.

Test Setup	Average Spray Pattern CV (%)	Average Nozzle Pressure CV (%)	Average Boom Section Pressure CV (%)	Average Nozzle Flow Rate CV (%)
Baseline	11.0	1.9	1.0	2.0
at 60% pressure	14.3	20.1	17.5	10.7
at 33% pressure	31.6	31.2	23.1	26.3

While spray pattern CV increased only 3.3% nozzle pressure CV, boom section pressure CV and flow rate CV increased 18.2%, 16.5% and 8.7%, respectively. This shows that spray pattern CV may not be as sensitive to blockages or restrictions as a nozzle flow rate or boom subsection pressure CV indication may be.

4.4.3 Full Boom Pressure, Flow and and System Based Estimates

In order to understand how system pressure and flow rate measurements relate to boom subsection pressure, a test was setup to measure the effects of an obstruction within a spray boom. A ball valve was plumbed into one boom supply line to two boom subsections on a sprayer. Four ball valve settings were recorded for the obstructed boom subsection: 100% flow, 95% flow, 85% flow and 0% flow. At each ball valve setting data were collected at four system pressure settings (207 kPa, 276 kPa, 345 kPa, and 414 kPa). The average and standard deviation of the pressure measurements throughout the tests are shown in Table 4.7.

Table 4.7: Observed average system pressure at each pressure setting and obstruction combination.

System Pressure Setting (kPa)	Average system pressure during test (kPa) [Standard deviation]			
	Boom subsections 3 & 4 restriction setting, percent of full flow			
	100%	95%	80%	0%
207	208.2 [2.10]	208.7 [1.60]	208.3 [1.70]	211.7 [1.58]
276	267.7 [1.57]	282.3 [1.79]	290.7 [1.72]	292.3 [1.73]
345	332.3 [1.62]	332.7 [1.59]	338.4 [1.63]	336.2 [1.79]
414	431.7 [1.56]	413.3 [1.51]	405.9 [1.49]	408.8 [1.62]

At each pressure setting, the obstruction was adjusted and pressure and flow rate data collected once steady state had been reached. During analysis, 5 minute samples of data were chosen once the system had reached steady state. At each combination of ball valve setting and system pressure, CAN bus flow rate and manual flow rate measurements were recorded. Manual flow rate estimates were recorded with a graduated cylinder and timer. Figure 4.17 shows flow rate estimates for one nozzle in each boom subsection (chosen at random) for all four pressure settings during the 80% of full flow obstruction setting. As shown, the nozzle flow rate for each pressure setting through the nozzles in boom subsections three and four remained at approximately 80% of the flow rates of the nozzles in the other boom subsections.

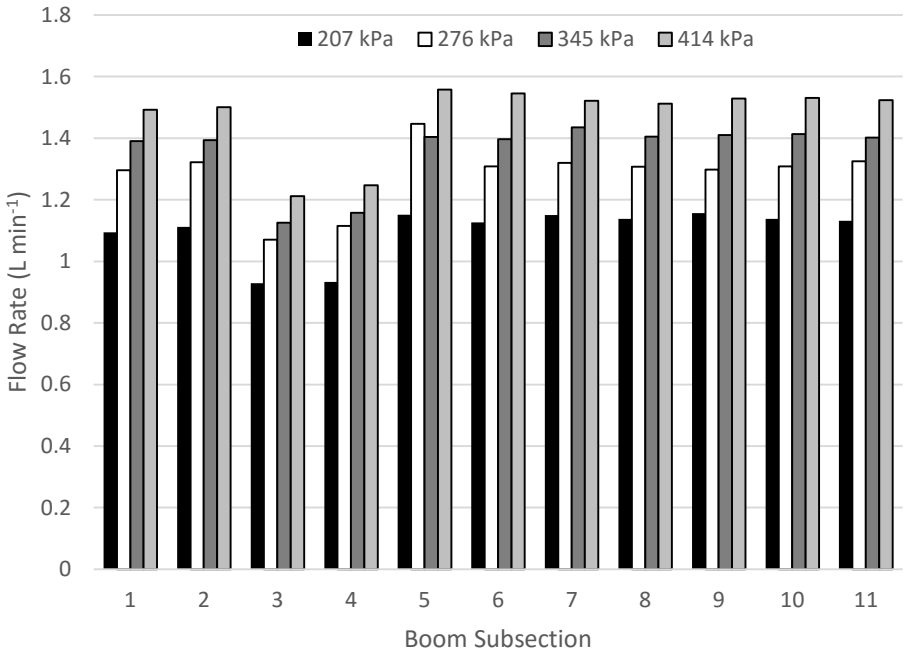

Figure 4.17: Hand recorded flow rate estimates from one nozzle in each subsection versus pressure at the 80% of full flow obstruction setting.

Flow rate values were also recorded from the CAN bus of the sprayer. Figure 4.18 shows CAN bus indicated flow rate values at of each pressure setting for each of the four obstruction settings. The 100% of full flow, 95% and 80% flow rate values were nearly indistinguishable from each other for all four pressure settings. However, with zero flow through boom subsections 3 and 4, the flow rates dropped across all four pressure settings.

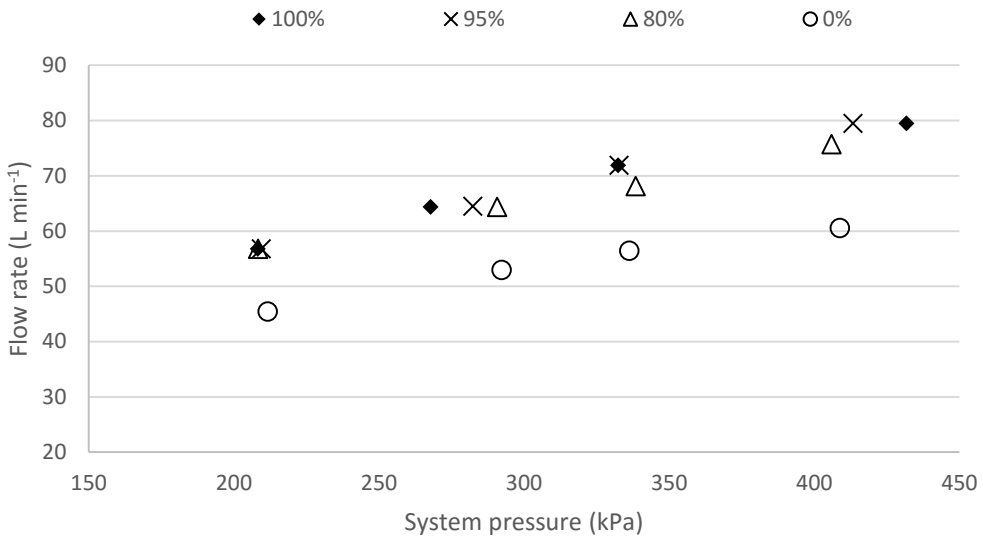

Figure 4.18: CAN bus indicated flow rate versus pressure for a flow obstruction test on an Apache AS715 self-propelled sprayer.

As flow to boom subsections 3 and 4 was reduced to zero, the flow rate values published to the CAN bus were reduced around 20% for each pressure setting (Figure 4.18). This shows that a blocked section could be detected if the flow rate dropped while pressure was maintained. These types of blockages could be detected for low flow from a section of nozzles, however, in situations where flow was blocked by less than 80%, flow rate measurements by a system flow meter may not have indicated it. In this case the flow

rate meter would not have indicated the blockage at 207 kPa or 276 kPa, but the lower flow rate may have been noticeable at 345 kPa and 414 kPa. The CAN bus indicated and hand measured flow rate values were compared (% difference) as shown in Table 4.8. Each of the flow rate values were within 7.0% for total flow rate of the system at each pressure and obstruction combination

Table 4.8: Percent difference between CAN bus indicated flow rate and hand measured flow rate estimates.

System Pressure Setting (kPa)	Percent difference between boom flow rate estimates (%)				
	Boom subsection restriction setting				Average
	100%	95%	80%	0%	
207	2.7%	6.9%	3.4%	2.0%	3.8%
276	1.7%	7.1%	6.7%	2.2%	4.4%
345	1.7%	2.4%	6.8%	0.5%	2.9%
414	3.1%	2.1%	4.1%	3.9%	3.3%
Average	2.3%	4.6%	5.3%	2.2%	

Nozzle flow rates for the full boom were calculated based on the system pressure and orifice equation 4.2 and compared to the CAN bus indicated flow rate (Table 4.9). The calculated flow rates were within 10% of the CAN bus flow rates for all four pressure settings at 100%, 95% and 80% flow rate settings. However, at 0% flow rate through subsections three and four the flow rate estimates differed an average of 39.2%.

Table 4.9: Percent difference between CAN bus indicated flow rate and system pressure based nozzle flow rates.

System Pressure Setting (kPa)	Percent difference between boom flow rate estimates (%)				
	Boom subsection restriction setting				Average
	100%	95%	80%	0%	
207	-9.3%	-9.2%	-9.3%	-30.9%	-14.6%
276	-8.7%	-5.9%	-4.0%	-38.9%	-14.4%
345	-6.9%	-6.9%	-0.7%	-42.1%	-14.1%
414	-0.3%	-3.2%	0.5%	-44.8%	-11.9%
Average	-6.3%	-6.3%	-3.4%	-39.2%	

Nozzle flow rates calculated from system pressure, with an obstruction, could be drastically different than actual system flow. To more closely estimate flow rate from pressure, nozzle flow rates were calculated based on individual boom subsection pressure, then summed to estimate system flow rate. These estimates were compared to the CAN bus indicated flow rates in Table 4.10. Comparing subsection pressure calculated flow rates to CAN indicated, the percent differences were less than 11%. The boom subsection based estimates averaged as high as -10.9% different than CAN indicated at 207 kPa and as low as -0.6% different at 414 kPa.

Table 4.10: Percent difference between CAN bus indicated flow rate and subsection pressure based nozzle flow rates.

System Pressure Setting (kPa)	Percent difference between boom flow estimates (%)				
	Boom subsection 4 restriction setting				Average
	100%	95%	80%	0%	
207	-7.6%	-8.0%	-10.9%	-9.3%	-9.0%
276	-7.1%	-4.9%	-6.5%	-7.6%	-6.5%
345	-5.4%	-6.1%	-3.6%	-5.8%	-5.2%
414	1.1%	-2.7%	-2.9%	-0.6%	-1.3%
Average	-4.8%	-5.4%	-6.0%	-5.8%	

These comparisons showed that flow estimates based on system pressure measurements can have very high error. When pressure was measured locally, flow rate estimates were much closer to the system flowrate measurements. Percent differences were calculated for each boom subsection between CAN bus indicated flow (proportioned to the number of nozzles in each boom subsection) and hand flow rate estimates for each boom subsection (Table 4.11 and

Table 4.12). For all four pressure settings (207 kPa, 276 kPa, 345 kPa and 414 kPa) at 100% of full flow, the subsection flow estimates were between -2.5% and 6.0%. However, in all pressure

settings the 0% flow differences were much higher, with the lowest difference being 16.3% and the highest difference being 28.1% (Table 4.11 and

Table 4.12). The trend in percent difference between CAN bus calculated boom subsection flow rate and hand estimated boom subsection flow rate shows how an obstruction or even a boom section turned off with section control could cause errors in flow rate calculation.

Table 4.13 and Table 4.14 show the results from comparing each boom subsection pressure based flow rate and the CAN bus indicated flow rate. Comparing subsection pressure based and CAN bus-indicated flow rates the restriction may be detected. If subsection pressure and flow rate were taken into account, a rate monitor may be able to detect obstructions as low as a 5% reduction from target flow rate.

Table 4.11: Percent difference of each boom subsection CAN bus calculated and hand flow rate estimates for 207 kPa and 276 kPa.

Boom Subsection	Percent difference in flow meter and nozzle flow estimates at 207 kPa (%)				Percent difference in flow meter and nozzle flow estimates at 276 kPa (%)			
	Boom section 4 restriction setting				Boom section 4 restriction setting			
	100%	95%	80%	0%	100%	95%	80%	0%
1	3.9%	5.7%	3.9%	21.3%	-1.6%	5.7%	8.1%	22.5%
2	4.7%	7.7%	5.4%	21.5%	6.0%	6.2%	9.9%	27.5%
3	0.0%	3.1%	-13.2%	-	-2.5%	2.7%	-11.4%	-
4	3.7%	6.1%	-12.7%	-	1.1%	6.0%	-6.9%	-
5	4.9%	8.6%	8.7%	28.1%	1.1%	8.5%	17.6%	25.9%
6	4.3%	7.1%	6.7%	24.6%	2.8%	7.2%	8.9%	24.9%
7	3.6%	8.0%	8.6%	24.8%	4.0%	6.8%	9.7%	23.8%
8	-0.7%	4.7%	7.6%	23.2%	2.1%	6.5%	8.9%	22.6%
9	1.6%	8.1%	9.1%	25.5%	1.8%	8.4%	8.2%	23.4%
10	1.4%	6.1%	7.6%	23.2%	0.7%	6.7%	8.9%	22.2%
11	3.3%	7.4%	7.1%	23.6%	2.8%	8.1%	10.1%	22.9%

Table 4.12: Percent difference of each boom subsection CAN bus calculated and hand flow rate estimates for 345 kPa and 414 kPa.

Boom Subsection	Percent difference in flow meter and nozzle flow estimates at 345 kPa (%)				Percent difference in flow meter and nozzle flow estimates at 414 kPa (%)			
	Boom section 4 restriction setting				Boom section 4 restriction setting			
	100%	95%	80%	0%	100%	95%	80%	0%
1	2.7%	1.4%	9.3%	16.3%	1.4%	2.2%	6.0%	23.3%
2	1.8%	2.4%	9.4%	21.1%	0.5%	1.8%	6.6%	24.6%
3	-1.9%	-0.9%	-12.1%	-	0.1%	-1.9%	-15.7%	-
4	0.7%	0.7%	-9.0%	-	2.3%	0.0%	-12.4%	-
5	2.6%	5.1%	10.1%	26.0%	5.0%	4.9%	10.0%	20.0%
6	2.7%	-2.6%	9.7%	23.5%	4.5%	3.6%	9.3%	26.2%
7	2.6%	6.4%	12.1%	24.3%	3.8%	-2.5%	7.9%	26.3%
8	1.5%	3.6%	10.2%	22.8%	3.9%	3.2%	7.3%	25.7%
9	1.0%	4.9%	10.6%	24.5%	3.0%	5.3%	8.3%	27.3%
10	1.0%	3.9%	10.7%	22.3%	3.2%	4.6%	8.4%	25.1%
11	3.4%	4.4%	10.0%	23.7%	4.3%	1.2%	8.0%	25.6%

Table 4.13: Percent difference of each boom subsection pressure based flow estimates and CAN bus-indicated flow rate at 207 kPa and 276 kPa.

Boom Subsection	Percent difference in flow meter and subsection pressure based flow estimates at 207 kPa (%)				Percent difference in flow meter and subsection pressure based flow estimates at 276 kPa (%)			
	Boom section 4 restriction setting				Boom section 4 restriction setting			
	100%	95%	80%	0%	100%	95%	80%	0%
1	7.0%	6.9%	7.0%	-18.4%	5.8%	3.3%	1.4%	-20.7%
2	7.6%	7.4%	7.5%	-16.8%	6.8%	4.3%	2.6%	-18.9%
3	7.4%	9.8%	22.6%	-	6.7%	7.1%	20.6%	-
4	7.4%	9.8%	22.6%	-	6.7%	7.1%	20.6%	-
5	7.6%	7.4%	7.5%	-16.5%	6.9%	4.3%	2.5%	-18.7%
6	7.6%	7.4%	7.5%	-16.5%	6.9%	4.3%	2.5%	-18.7%
7	7.6%	7.4%	7.5%	-16.5%	6.9%	4.3%	2.5%	-18.7%
8	7.8%	7.5%	7.6%	-16.3%	7.1%	4.4%	2.6%	-18.6%
9	8.1%	7.6%	7.7%	-16.2%	7.3%	4.5%	2.7%	-18.4%
10	7.6%	7.3%	7.3%	-16.5%	7.0%	4.2%	2.5%	-18.8%
11	8.7%	8.2%	8.2%	-15.7%	7.8%	5.0%	3.2%	-18.0%

Table 4.14: Percent difference of each boom subsection pressure based flow estimates and CAN bus-indicated flow rate at 345 kPa and 414 kPa.

Boom Subsection	Percent difference in flow meter and subsection pressure based flow estimates at 345 kPa (%)				Percent difference in flow meter and subsection pressure based flow estimates at 414 kPa (%)			
	Boom section 4 restriction setting				Boom section 4 restriction setting			
	100%	95%	80%	0%	100%	95%	80%	0%
1	3.9%	4.1%	-2.5%	-23.2%	-3.2%	0.1%	-3.8%	-30.2%
2	5.4%	5.5%	-0.9%	-21.2%	-1.0%	2.1%	-1.8%	-27.7%
3	5.3%	8.5%	19.1%	-	-1.0%	5.4%	19.5%	-
4	5.3%	8.5%	19.1%	-	-1.0%	5.4%	19.5%	-
5	5.5%	5.5%	-0.8%	-21.0%	-0.9%	2.0%	-1.7%	-27.6%
6	5.5%	5.5%	-0.8%	-21.0%	-0.9%	2.0%	-1.7%	-27.6%
7	5.5%	5.5%	-0.8%	-21.0%	-0.9%	2.0%	-1.7%	-27.6%
8	5.6%	5.6%	-0.7%	-20.9%	-0.9%	2.1%	-1.7%	-27.5%
9	5.8%	5.8%	-0.6%	-20.9%	-0.8%	2.2%	-1.5%	-27.4%
10	5.6%	5.6%	-0.8%	-21.1%	-1.3%	2.0%	-1.8%	-27.7%
11	6.4%	6.1%	0.0%	-20.4%	-0.7%	2.6%	-1.1%	-26.8%

4.5 Conclusions

Laboratory patternator test results indicated that nozzle flow rate or pressure (when downstream of an obstruction) measurements indicated system disturbances to a greater degree than pattern CV estimates. Spray pattern CV estimates did not indicate significant changes in uniformity until nozzle flow rates (XR and AIXR nozzles) had been reduced by over 20% of the desired rate.

When laboratory pattern data were used to simulate a full boom tested under similar conditions, comparisons indicated that changes in spray pattern uniformity responded similarly to boom obstructions. Taking into account nozzle lateral angle changes on the full boom sprayer, spray pattern simulations produced similar CVs as full boom pattern testing. These results showed that changes in CV could be simulated using laboratory pattern data. Results of full boom patternator testing supported laboratory findings that boom flow and pressure measurements may be more sensitive to detecting obstructions in boom flow.

Comparisons among system pressure and flow measurements versus sub-section measurements indicated that system estimates may not provide an accurate depiction of actual boom distribution. A pressure based flow rate estimation indicated flow rates much lower than CAN bus indicated flow rates. Subsection pressure based flow estimates and CAN bus-indicated flow rates may indicate obstructions as little as 5% below target rate in a boom subsection.

Chapter 5. Summary and Future Utilization of this Project

The data acquisition system was designed to help aid in data collection for creating “as-applied” maps for pesticide and nutrient application. The system could easily adapt an analog flow rate meter to verify the CAN bus flow rate measurements and log pressure and flow rates as a sprayer operates to improve as-applied maps to provide detail to the subsection level. Subsection pressure reflected flow rate differences that system pressure could not detect. The combination of boom subsection pressure and system flow rate could improve the accuracy of as-applied maps.

References

ASABE Standards. (2011). S592: Best Management Practices for Boom Spraying. *St. Joseph, MI: ASABE*.

ASTM. (2006). Standard Methods for Testing Hydraulic Spray Nozzles Used in Agriculture. *E641-01*.

Azimi, A., Carpenter, T., & Reichard, D. (1985). Nozzle spray distribution for pesticide application. *Transactions of the ASAE-American Society of Agricultural Engineers (USA)*.

Bosch, R. (1991). CAN specification version 2.0. *Rober Bousch GmbH, Postfach* 300240.

Gebhardt, M. R., Day, C. L., Goering, C. E., & Bode, L. E. (1974). Automatic Sprayer Control System. *Transactions of the ASAE*1043-1047.

Grisso, R. D., Hewett, E. J., Dickey, E. C., Schnieder, R. D., & Nelson, E. W. (1988). Calibration Accuracy of Pesticide Application Equipment. *Applied Engineering in Agriculture* 4(4): 310-315.

Grisso, R., Jasa, P., & Rolofson, D. (2002). Analysis of traffic patterns and yield monitor data for field efficiency determination. *Applied Engineering in Agriculture* 18(2): 171.

Grisso, R. D., Kocher, M. F., Adamchuk, V. I., Jasa, P. J., & Schroeder, M. A. (2004). Field efficiency determination using traffic pattern indices. *Applied Engineering in Agriculture* 20(5): 563.

Klein, R. N. (2004). Spray Boom Set-up on Field Sprayers. *University of Nebraska-Lincoln Extension Publicaion* http://extensionpubs.unl.edu/publication/9000016367829/spray-boom-set-up-on-field-sprayers/.

Luck, J. D., Schaardt, W. A., Sharda, A., & Forney, S. H. (2016). Development and Evaluation of an Automated Spray Patternator Using Digital Liquid Level Sensors. *Applied Engineering in Agriculture* 3247-52.

Luck, J. D., Zandonadi, R. S., Luck, B. D., & Shearer, S. A. (2010a). Reducing Pesticide Over-application with Map-Based Automatic Boom Section Control on Agricultural Sprayers. *Transactions of the ASAE-American Society of Agricultural Engineers (USA)* 53(3): 685-690.

Luck, J., Sharda, A., Pitla, S., Fulton, J., & Shearer, S. (2011a). A case study concerning the effects of controller response and turning movements on application rate uniformity with a self-propelled sprayer. *Transactions of the ASABE* 54(2): 423-431.

Luck, J., Pitla, S., Shearer, S., Mueller, T., Dillon, C., Fulton, J., & Higgins, S. (2010b). Potential for pesticide and nutrient savings via map-based automatic boom section control of spray nozzles. *Computers and Electronics in Agriculture* 70(1): 19-26.

Luck, J. D., Pitla, S. K., Zandonadi, R. S., Sama, M. P., & Shearer, S. A. (2011b). Estimating off-rate pesticide application errors resulting from agricultural sprayer turning movements. *Precision Agriculture* 12(4): 534-545.

Mawer, C. J., &Miller, P. C. H. (1989). Effect of roll angle and nozzle spray pattern on the uniformity of spray volume distribution below a boom. *Crop Protection* 8(3): 217.

National Instruments. (2014). Getting Started with LabVIEW. *Austin, Texas: National Instruments* 2012.

Ozkan, H., &Ackerman, K. (1992). An automated computerized spray pattern analysis system. *Applied engineering in agriculture (USA)*.

Ozkan, H., Reichard, D., & Ackerman, K. (1992). Effect of orifice wear on spray patterns from fan nozzles. *Transactions of the ASAE*.

Porter, W., Rascon, J., Shi, Y., Taylor, R., & Weckler, P. (2013). Laboratory Evaluation of a Turn Compensation Control System for a Ground Sprayer. *Applied Engineering in Agriculture*.

SAE. (2000). Serial Control and Communications Heavy Duty Vehicle Network J1939.

SAS Institute Inc. (2013). SAS/CONNECT 9.4 User's Guide, Second Edition. *Cary, NC: SAS Institute Inc.* 9.4.

Sharda, A., Fulton, J. P., McDonald, T. P., & Brodbeck, C. J. (2011). Real-time nozzle flow uniformity when using automatic section control on agricultural sprayers. *Computers and Electronics in Agriculture* 79(2): 169-179.

Sharda, A., Luck, J. D., Fulton, J. P., McDonald, T. P., & Shearer, S. A. (2013). Field application uniformity and accuracy of two rate control systems with automatic section capabilities on agricultural sprayers. *Precision Agriculture* 14(3): 307-322.

Sharda, A., Fulton, J. P., McDonald, T. P., Zech, W. C., Darr, M. J., & Brodbeck, C. J. (2010). Real-Time Pressure and Flow Dynamics due to Boom Section and Individual Nozzle Control on Agricultural Sprayers. *Transactions of the Asabe* 53(5): 1363-1371.

Smith, V. H., Tilman, G. D., & Nekola, J. C. (1999). Eutrophication: impacts of excess nutrient inputs on freshwater, marine, and terrestrial ecosystems. *Environmental pollution* 100(1): 179-196.

Stone, M. L., Benneweis, R. K., & Bergeijk, J. V. (2008). Evolution of Electronics for Mobile Agricultural Equipment. *Transactions of the ASAE-American Society of Agricultural Engineers (USA)* 51(2): 385-390.

TeeJet Technologies. (2015). Broadcast Nozzles Selection Guide. *http://www.teejet.com/spray_application/nozzles.shtml*8-13.

USDA. (2016). Farm Income and Wealth Statistics. Available at: http://www.ers.usda.gov/data-products/farm-income-and-wealth-statistics/production-expenses.aspx?reportPath=/FarmIncome/FarmIncomeWeb_201605/PE_State_US&EXtype=All expenses&decade=2010&ValueTerm=N. Accessed 05/26 2016.

USDA. (2012). 2012 Census of Agriculture, United States, Summary and State Data. Available at: https://www.agcensus.usda.gov/Publications/2012/Full_Report/Volume_1,_Chapter_1_US/. Accessed 6/30 2015.

Younes, M., &Galal-Gorchev, H. (2000). Pesticides in drinking water—a case study. *Food and chemical toxicology* 38S87-S90.

Appendix 1: LabVIEW VI for analog and CAN bus data collection

The LabVIEW Virtual Instrument (VI) created to log CAN bus and analog data simultaneously through National Instruments modules.

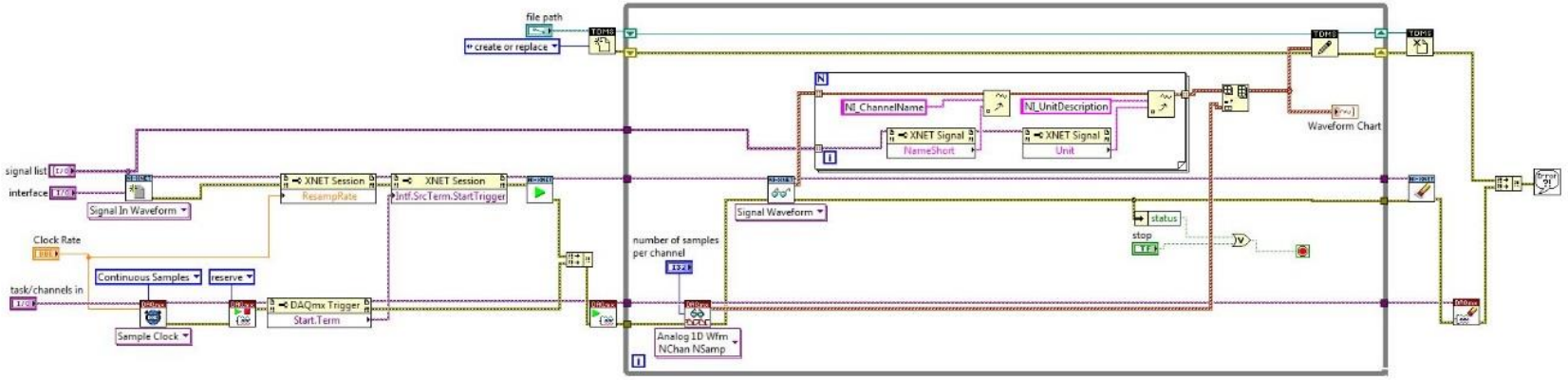

Appendix 2: Arduino code for analog pressure data collection

```
void setup()

{

  Serial.begin(9600);          //  setup serial

}

void loop()

{

 float AN0 = analogRead(0); //stores analog values in floats
 float AN1 = analogRead(1);
 float AN2 = analogRead(2);
 float AN3 = analogRead(3);
 float AN4 = analogRead(4);
 float AN5 = analogRead(5);
 float AN6 = analogRead(6);
 float AN7 = analogRead(7);
 float AN8 = analogRead(8);
 float AN9 = analogRead(9);

 float SENSOR0 = AN0 / 1023 *100.00 ;//converts analog to psi
 float SENSOR1 = AN1 / 1023 *100.00 ;
 float SENSOR2 = AN2 / 1023 *100.00 ;
 float SENSOR3 = AN3 / 1023 *100.00 ;
 float SENSOR4 = AN4 / 1023 *100.00 ;
 float SENSOR5 = AN5 / 1023 *100.00 ;
 float SENSOR6 = AN6 / 1023 *100.00 ;
 float SENSOR7 = AN7 / 1023 *100.00 ;
 float SENSOR8 = AN8 / 1023 *100.00 ;
 float SENSOR9 = AN9 / 1023 *100.00 ;

 Serial.print(SENSOR0);
 Serial.print(",");
  Serial.print(SENSOR1);
 Serial.print(",");
  Serial.print(SENSOR2);
 Serial.print(",");
  Serial.print(SENSOR3);
 Serial.print(",");
  Serial.print(SENSOR4);
 Serial.print(",");
  Serial.print(SENSOR5);
 Serial.print(",");
  Serial.print(SENSOR6);
 Serial.print(",");
  Serial.print(SENSOR7);
 Serial.print(",");
  Serial.print(SENSOR8);
 Serial.print(",");
  Serial.println(SENSOR9);

delay(1000);
}
```

Appendix 3: SAS code for least significant means test

```
data water;
  input nozzle angle cv;
CARDS;
8003  0     4.1
8003  0     3.7
8003  0     4.7
;
proc print data=water; run;

proc univariate data=water;
  var cv;
  histogram;
run;
ods graphics on;
ods html select all;
/* treating angle as discrete */
proc glimmix data=water plot=residualpanel;
  class nozzle angle ;
  model cv = angle;
  lsmeans angle / diff lines plot=meanplot(join cl);
run;
/* treating angle as discrete */
/* using a control adjustment */
proc glimmix data=water plot=residualpanel;
  class nozzle angle ;
  model cv = angle;
  lsmeans angle / diff=control('0') adjust=dunnett lines
plot=meanplot(join cl) ;
run;
/* Treating angle as cont. */
proc glimmix data=water plot=residualpanel;
  class nozzle;
  model cv = angle / solution;
  *lsmeans angle / diff lines plot=meanplot(join cl);
run;
```